PRATHAM

IIT BOMBAY STUDENT SATELLITE

Preliminary Design Report

Power System

By

Ameya Damle

Mehul Tikekar

Chiraag Juvekar

Akshay Bedhotiya

Garvit Junival

Department of Aerospace Engineering,

Indian Institute of Technology, Bombay

April, 2009

1. Introduction

This document contains the preliminary design of the electrical power supply of Pratham, IIT Bombay's student satellite. It details the main requirements, design and analysis of the power system of the satellite. It contains results of simulation and actual testing of circuits that was done over the past year, the inferences drawn from the results and the decisions taken on their basis.

1.1. Requirements of PS

The main requirements placed upon the power supply (*PS*) of the satellite can be stated as follows:

To provide electrical power as per demands of the other subsystems.

To collect data of the health of the power system and send it to the on-board computer (*OBC*) for down linking.

It is a completely autonomous system which collects power from sources, stores it and distributes it to the various electrical loads. Hence, a list of all the functions can be made.

1.2. Functions of PS

1. To collect solar power.
2. To supply power to various electronic circuits as required.
3. To store the excess power available.
4. To monitor condition of each load.
5. To switch off a load if it is malfunctioning or not in use.
6. To store all voltage, current and temperature values indicating the health of the PS and relay this information to the OBC
7. To power-up the satellite upon ejection from the launch vehicle

2. Power Budget

The power budget is a calculation of the total power requirements of the various subsystems and the total power input from various sources.

2.1. Power requirements

The other satellite subsystems and their functions are explained in brief.

Payload (*PAY*) – The satellite mission is to measure the total electron count (*TEC*) in the ionosphere. This is accomplished by sending a linearly polarized radio wave from the satellite to the ground station. In the process, the plane of polarization of the wave rotates by an angle proportional to the amount of free electrons in the medium it traversed through. This angle is measured to give the TEC.

Communication (*COM*) – Responsible for communication between the satellite and ground station. The satellite has a beacon and a communication downlink both of which are utilized by the payload. No uplink has been planned for this satellite.

Attitude determination and control system (*ADCS*) – Controls the orientation of the satellite in space to ensure that the antennae point in a particular direction. The attitude is determined by various sensors like magnetometer, sun-sensors, GPS and rate gyroscopes. Control is achieved using magnetotorquer coils which provide torque depending on the current passing through them.

On-board computer (*OBC*) – Handles information to be transmitted and interfaces with the sensors and actuators for the ADCS.

Structures and thermals (*ST*) – Looks after the proper placement of all components on the satellite to ensure that they are operated in their safe operation conditions.

The power requirements of all the various subsystems are given below.

Circuit	Energy consumed (W-hr)
Beacon	12.023
Downlink	3.410
GPS	7.200
Gyroscopes	0.420
Sun Sensors	1.200
Magnetometer	5.760
Magneto-torquer	12.420
Torquer driver	0.390
OBC	23.760
Battery Heater	28.889
Total	95.472

Table 1: Power Budget

With losses in power circuit this figure goes to 120W-hrs.

When the satellite passes over ground station while in eclipse, this condition requires maximum power from battery, which is 5.33 W-hrs.

2.2. Power sources

The main sources of power for a space mission are solar power, chemical power (non-rechargeable cells, fuel cells) and nuclear power. Chemical power is suitable only for short missions and nuclear power is suitable only for large missions with large power requirements. For small satellites like Pratham, with a designed lifetime of a few months to a few years, solar power is the most suitable source of power. Recent advancements in solar cell technology make it possible to harness Sun's energy with considerable efficiency (around 25%). Newer cells based on Gallium Arsenide (GaAs) have higher efficiencies as compared to Silicon (Si) cells and also degrade slower in the harsh space environment.

2.2.1. Incident radiation

The satellite receives light from three sources: Direct solar radiation, Sunlight reflected from Earth and Earth's thermal radiation. Direct solar radiation is the major component of these. Power available from solar radiation is calculated analytically.

The total useful power on each of the faces is found to be:

A	A’	B	B’	C	C’	Total
14W	1W	10W	8W	12W	0W	45W

Table 2: Solar Power Incident

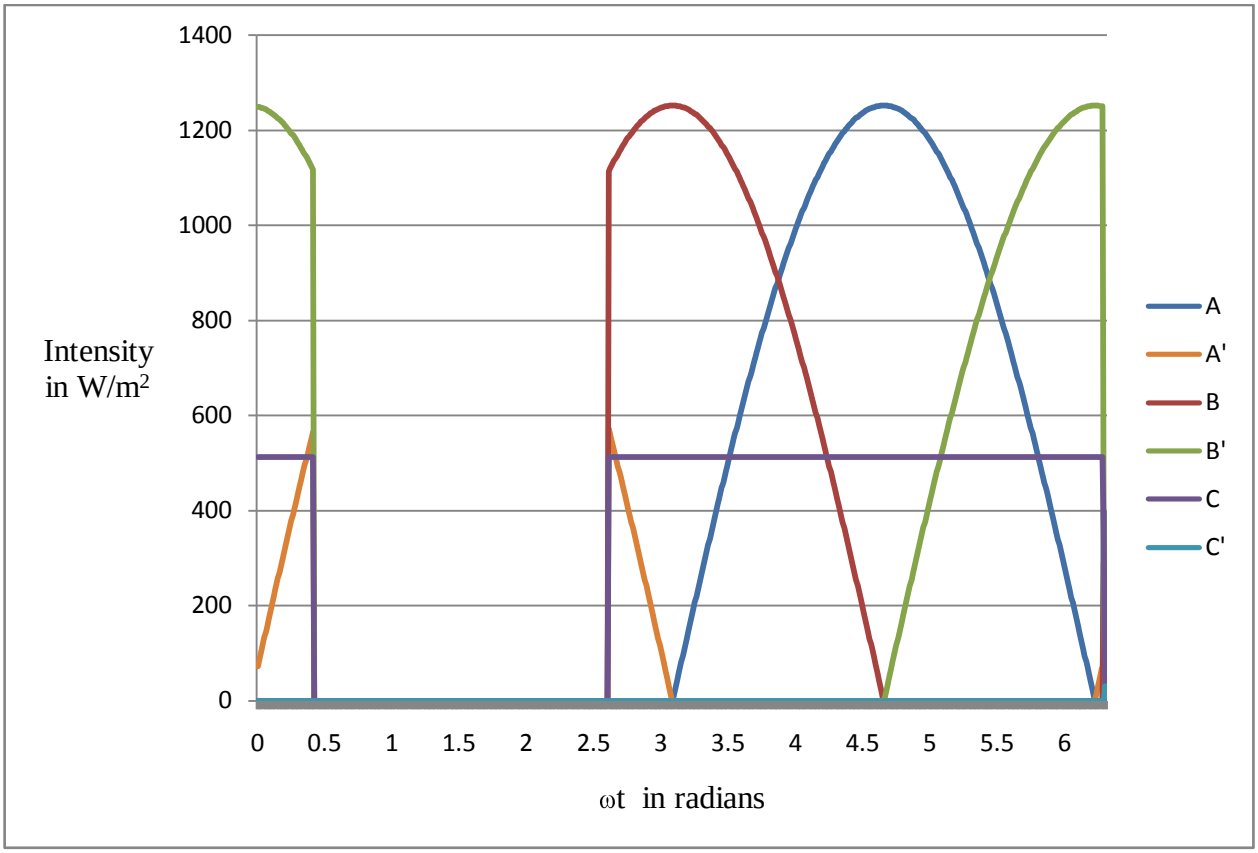

Detailed Calculations are attached.

Albedo also contributes to solar flux incident. This flux was also calculated. But, it has not been included in further calculations.

3. Space Radiation Dose

Space environment consists of charged particles such as electrons and protons of varied energies. Their effect on the satellite components can be critical and hence, the components must be simulated and tested for radiation.

3.1 Sources and effects of damaging radiation

The main sources of radiation are the trapped particles in the Earth's magnetic field. Trapped electrons with energies up to 7 MeV and protons with as much as 500 MeV energy are found in the inner Van Allen belts which extend from 700 km to 10,000 km in altitude. As the Earth's magnetic axis is inclined to the rotational axis, the Van Allen belt reach close to 200 km at regions over the South Atlantic Ocean. This effect, called the South Atlantic Anomaly, is a potential source of radiation dose for our satellite. Other high energy particles like neutrons, alpha particles, and UV, X-ray and gamma radiation also cause unpredictable operation of space electronics and degradation of their electrical parameters over time.

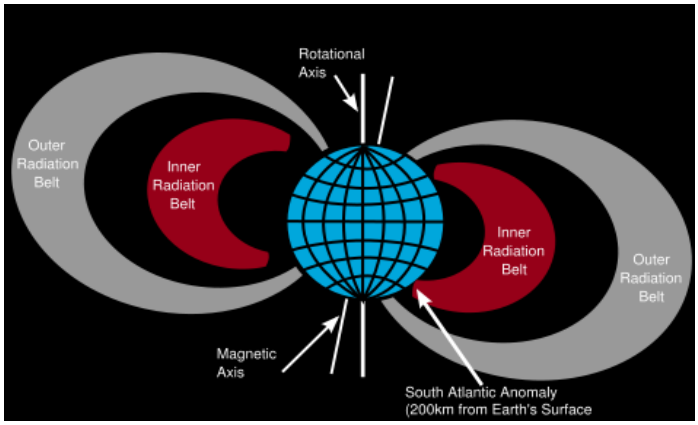

Figure 1: Van Allen belts. Courtesy: Wikipedia

Radiation is measured in two units: neutrons/cm^2 and radiation absorbed dose (rad). The first one is the amount of radiation dose equivalent to an exposure to a collimated beam of a specified number of neutrons per square centimeter having energy of 1 MeV while the second one is the amount of radiation dose causing 0.01J energy to be absorbed by 1kg of the specified matter.

The effects of damaging radiation can be classified as displacement damage and ionization damage. Another type of effect is related to the rate at which radiation is absorbed by the circuits. These include single event effects (SEE) like latch up, bit flips, burn out and snap back caused by a high energy particle creating a trail of ionization inside the bulk of the semiconductor.

Bipolar devices are usually susceptible to displacement damage while ionization damage is more pronounced in MOSFET devices. Most of the electronic devices suffer from single event effects due to the high energies of the incident particles. While special fabrication technologies are required to make radiation hardened ICs, it is possible to design commercial circuits such that the effect of radiation is reduced.

3.2 Simulations

Simulations for effects of radiation on the satellite have been carried out using SPENVIS, the Space Environment Information System by ESA. It is a WWW interface to models of the space environment and its effects. SPENVIS requires a specified orbit to calculate the effects of space weather on it. The following orbit parameters have been used for further simulations –

a. Orbit type: heliosynchronous

b. Eccentricity: 0.00

c. Semi major axis: 7048.16 km

d. Local time on earth at satellite's nadir: 10.30

e. Inclination: 98.07°

f. Period: 1.64 hrs

g. Mission duration: 365.00 days (1.00 years)

Various models have been implemented in SPENVIS for simulating the trapped protons and electrons and their effects for a particular orbit. The entire simulation procedure can be split into the following steps:

3.1 Trapped electrons and protons

3.2 Damage equivalent fluences for solar cells

3.3 Ionising doses

3.2.1 Trapped electrons and protons

The Air Force Research Laboratory (AFRL) (www.vs.afrl.af.mil) has developed two models for the trapped proton and trapped electron environments as seen by the CRRES satellite: CRRESPRO [*Meffert and Gussenhoven*, 1994] for protons, and CRRESELE [*Brautigam and Bell*, 1995] for electrons, respectively. These models are available from the authors, and have been included in AFRL's GEOSPACE software package. With permission from AFRL, the flux maps for these models have been included in the SPENVIS trapped radiation tool, in the framework of the ESA/ESTEC sponsored TREND (TRapped Radiation ENvironment Development) project. These are the latest models for trapped electrons and protons implemented in SPENVIS. These models were used to simulate the trapped radiation under two different conditions-

Quiet solar behaviour: The peak proton flux above 10 MeV came out to be 1.19×10^4 protons per sq.cm. per second. The peak electron flux above 3 MeV came out to be 1.02×10^1 electrons per sq.cm. per second.

Active solar behaviour: The peak proton flux above 10 MeV came out to be 1.05×10^4 protons per sq.cm. per second. The peak electron flux above 3 MeV came out to be 2.85×10^4 electrons per sq.cm. per second.

3.2.2 Damage equivalent fluences for solar cells

The EQFLUX program, developed by the Jet Propulsion Laboratory (JPL) calculate 1 MeV and 10 MeV damage equivalent electron and proton fluences, respectively, for exposure to the fluences predicted by the trapped radiation and solar proton models, for a specified duration. These fluences can then be simulated in the laboratory environment.

The simulations were carried out for the Spectrolab 3J multijunction cells. The radiation models used for electron and proton fluences were the same as in section 3.1 of this document.

Assuming no cover glass over the solar cells, the 1 MeV equivalent electron fluences incident on the solar panels per sq. cm. of exposed area over one year were-

a. Quiet solar behaviour - 2.56×10^{14}

b. Active solar behaviour - 3.22×10^{14}

For this radiation, the Spectrolab Triple Junction (TJ) solar cell suffers a degradation of 8%.

3.2.3 Ionising Dose

SHIELDOSE [*Seltzer*, 1980] is a computer code for space-shielding radiation dose calculations. It determines the absorbed dose as a function of depth in aluminum shielding material of spacecraft, given the electron and proton fluences encountered in orbit. SHIELDOSE-2 [*Seltzer*, 1994] differs from SHIELDOSE mainly in that it contains new cross sections and supports several new detector materials, and has a better treatment of proton nuclear interactions.

The radiation models used for electron and proton fluences were the same as in section 3.1 of this document. The thickness of finite aluminum slab shielding the components inside the satellite was assumed to be 2 mm. The following total ionising doses over the period of one year were obtained from the SHIELDOSE-2 model-

a. Quiet solar behavior - 0.718 Krad

b. Active solar behavior – 30.93 Krad

It is of importance to note that most commercial-grade electronics frequently survives up to 30 Krad with or without degradation in performance. Currently, efforts are being taken to understand the simulation of single event effects.

3.3 Choosing components

Most commercial components can be expected to perform without significant degradation during the designed lifetime of the satellite. However, some general rules and tips can be considered such as:

1. Use tested components (components with space heritage) or components made on same assembly line as tested ones
2. Use ROM for storing data.
3. For power MOSFETs, use rad-hard parts or keep generous margins
4. Run microcontroller at less than rated frequency
5. Use shielding (aluminum, tantalum, high-Z metals)
6. Redundancy (not useful for all technologies)
7. Robust electronic design. High drive currents, low fan-out or loading. Large gain margins, high noise immunity
8. Fault tolerant design
9. Error detection and correction
10. Ensure that system can reboot autonomously (watchdog)
11. Database of radiation testing. e.g. Comrad-UK
12. Use same Lot-Date code for test and flight hardware

13. Get components list reviewed by radiation expert (e.g. BARC, TIFR, ISRO scientists)
14. Some commercial ICs are inherently tolerant to radiation. eg. TTL logic, diodes, microwave devices, crystals and most passives

4. Maximum Power Point Tracking of Solar Panels

Maximum power point tracking involves actively varying the voltage and current of the solar panel so as to draw maximum power from them.

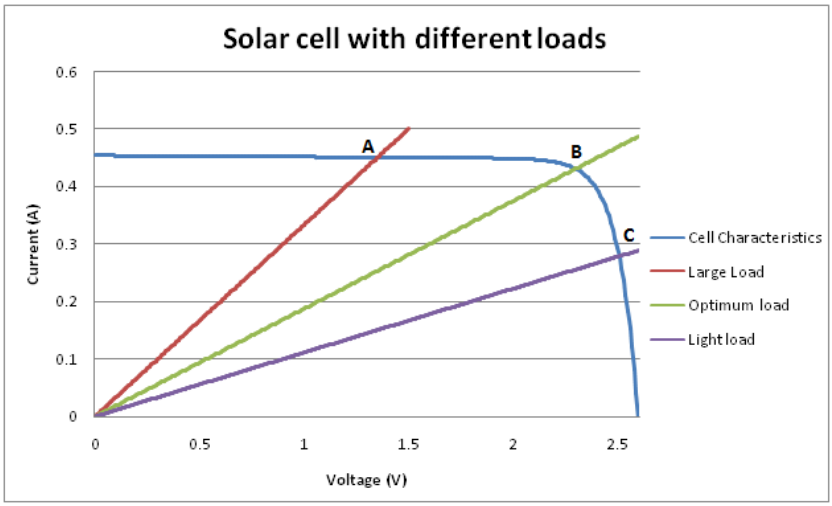

Figure 2: Solar cell with different loads at constant illumination

At the optimum point of operation B, maximum power can be extracted from the cell. This can be seen following graph of the power generated by the solar cell versus its operating voltage. Thus, the objective of MPPT circuit is to ensure that the solar cell always operates at the point of maximum power. This maximum power point (MPP) shifts with varying illumination and temperature of the cell. This variation can be seen in the following P-V graph for a solar cell at different illuminations and temperatures.

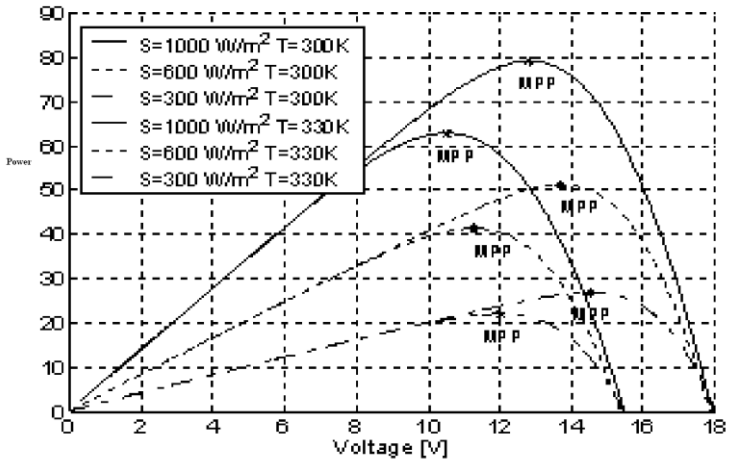

Figure 3: Solar power generated at different illuminations and temperatures

With MPPT:

Assuming that the MPPT circuit has 90%, the power obtained after MPPT

P = Sum of average solar radiation falling on each panel * Effective solar panel area * Solar cell efficiency *MPPT efficiency

= (398 + 291 + 291 + 334) W/m^2 *319.2 * 10^(-4) m^2 * 0.275 * 0.9

= 10.38 W

For a 95% efficient MPPT, this number rises to 10.95W and for an 85% efficient MPPT, it is 9.80W.

With the proposed method:

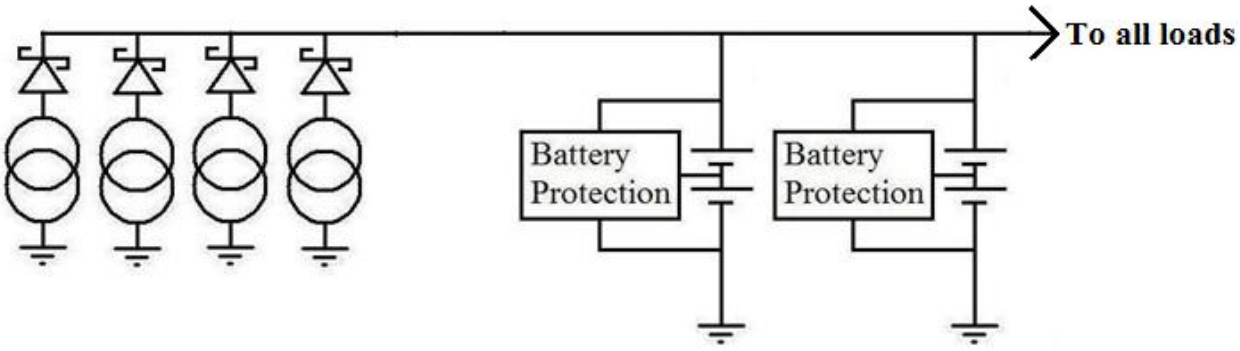

Since the depth of discharge of the battery is about 6%, the battery voltage varies from 8V to 8.2V. For the purpose of calculations, the battery is assumed to be at a constant 8.1V. Since the schottky diodes have a drop of 0.3V, the solar panels are at 8.4V.

At 1353 W/m^2, the solar panels have V_{OC} = 10.4V, V_{MP} = 9.2V and I_{SC} = 1.362A. From the I-V characteristics of the solar cells, it is found that at 8.4V, the current is approximately 1.35A which is 22mA less than the short circuit current. At lower intensities, the I-V curve shifts downwards. So, the current at 8.4V is always less than the corresponding short circuit current by 22mA. Considering this, the currents generated by each solar panel are found.

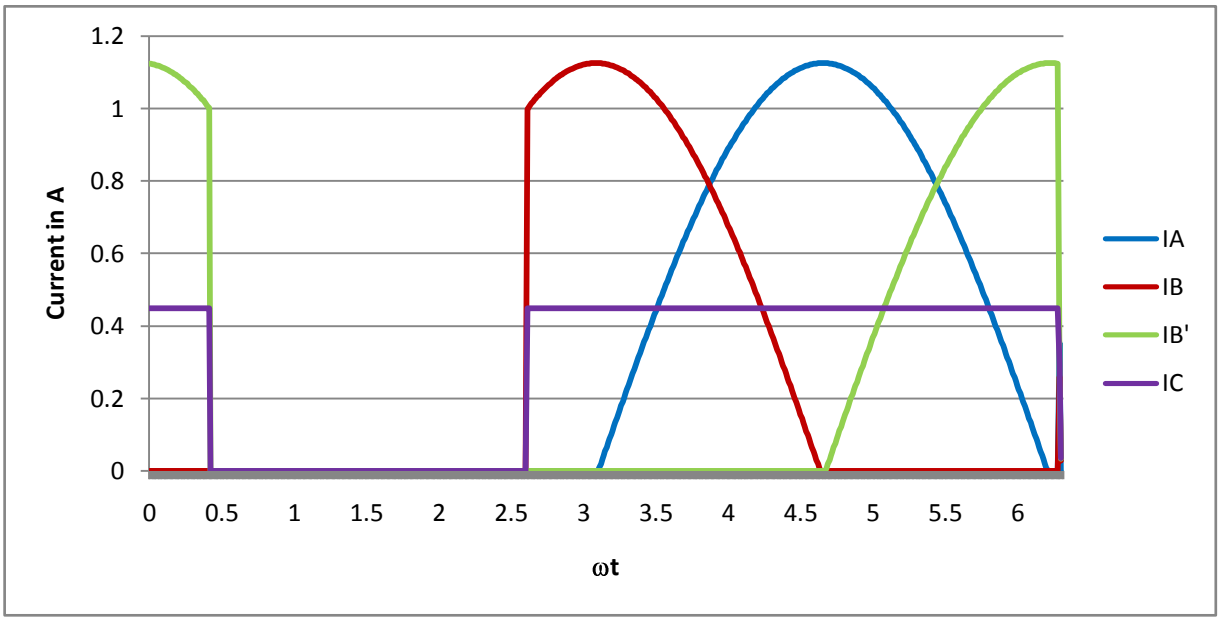

The average currents are I_A = 0.354A, I_B=0.259A, $I_{B'}$ = 0.259A and I_C = 0.292A. The total average current is 1.166A. Since this current is being supplied to the battery bus at 8.1V, the total power transferred after the diodes is 9.44W.

Hence, the total power gain due to using MPPT is somewhere between 0.4W and 1.5W.

The most recent power requirements are about 5W. The power distribution circuits involve regulators for 3.3V and 5V bus and OR-ing diodes. Assuming 10% losses in the regulators and 10% loss in the diodes, we are required to provide 6.25W. Hence, the gain provided by MPPT is not needed. The above mentioned charging method has been selected considering its simplicity and lower chances of failure.

For future reference, if the solar panel temperature changes or the battery depth of discharge changes, we have created a table showing the power transferred to the battery bus as a function of the battery voltage and solar panel V_{MP}. The power transferred is given as a percentage of the maximum power that could be transferred in an ideal case of a 100% efficient MPPT circuit.

	Battery Voltage				
V_{MP} of solar panel	**6.5 V**	**7.1 V**	**7.7 V**	**8.1 V**	**8.3 V**
10.8 V	**63%**	**69%**	**74%**	**78%**	**80%**
10.0 V	**68%**	**75%**	**80%**	**83%**	**85%**
9.2 V	**74%**	**81%**	**87%**	**91%**	**92%**
8.4 V	**81%**	**88%**	**92%**	**96%**	**80%**
7.6 V	**89%**	**93%**	**64%**	**32%**	**0%**

Table3: Power transfer efficiency without MPPT

The yellow and green cells are for > 80% efficiency and are the most desirable operating conditions.

5. Flight Hardware

We now describe the hardware to be used on the satellite.

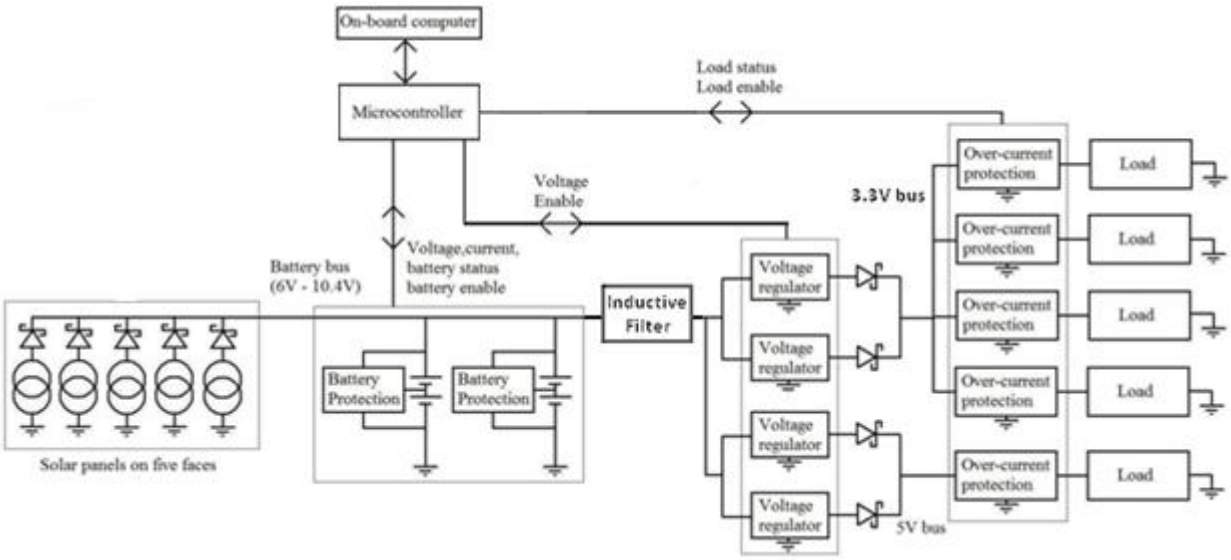

Figure 4: Flight hardware

Five solar panels with reverse blocking diodes are connected to the battery bus. The batteries are connected in a 2-series 2-parallel configuration for redundancy and have protection circuits on them. Voltage regulators step down the battery voltage to 5V and 3.3V. There are current limiting switches in series with each load to ensure shut-down in case of excessive power drawn by that particular load.

5.1 Solar cells

The satellite is powered by solar panels on four faces. One of the side faces is reserved for the antennae and another for launch vehicle interface.

Solar cells will be provided by ISRO. Rough values of characteristics of solar cells are as follows

- V_{OC} = 1010 mV
- V_{MP} = 870 mV
- $_{ISC}$ = 260 mA
- I_{MP} = 235 mA
- Maximum efficiency = 18%
- Dimensions: 20.25mm(±0.05mm) X 40.25mm(±0.05mm)

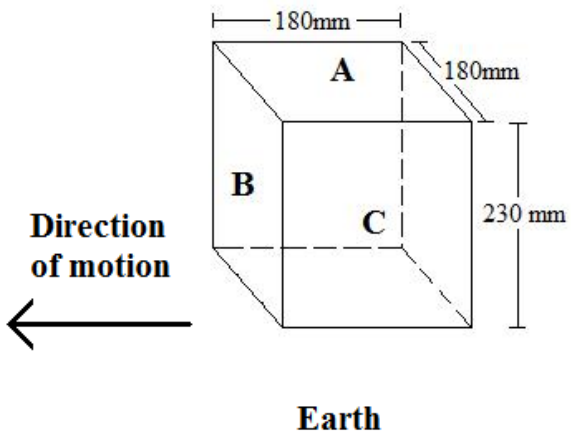

Figure 5: Satellite motion

5.2 Solar Panel:

The faces A, B, C will have 44 cells each and the face B' has 33 cells to make space for GPS antenna. All faces have the cells connected in strings of eleven cells in series. Hence, faces A, B, C have 4 such strings while the B' face has 3 such strings. Since no sunlight ever falls on the face C', that face has been used for the antennae and the launch vehicle interface.

Thus, the voltage ratings of all the panels are the same: V_{OC} = 11.1V and V_{MP} = 9.57V. Panels are designed to have such high V_{MP} because at higher temperature this value falls. Since, MPPT is not used, if V_{MP} falls below battery voltage, very low power output. The maximum temperature of the solar panels is calculated by the thermals team to be around 35° C. Hence we shall assume room temperature values for all subsequent calculations.

Solar panels will be fabricated by ISRO as per specifications required. 10mm Aluminum honeycomb is proposed to be used as base for the panel. Size of the panels will be approximately 22cm x 22cm.

5.3 Battery pack

Rechargeable lithium-ion technology has been selected for the satellite considering their superior performance and characteristics over the other battery technologies like nickel cadmium (NiCd) and nickel metal hydride (NiMH). 18650 cylindrical Lithium Ion cells are chosen. The cells will be provided by ISRO. Above mentioned cells have the following characteristics:

They will be assembled into a 2-series 2-parallel pack. Thus, the total rating of the battery is:

- Mean voltage = 7.2V
- Guaranteed capacity = 5 Ah
- Energy = 37 Wh
- Depth of discharge = 6%
- For a power consumption of around 5W, the satellite can run for around 7 hours without solar power on a full battery.

The battery specifications can be seen in detail in the following figures.

Model ICR18650 B2		
0.2C Capacity *	Nominal	2600 mAh
	Minimum	2500 mAh
Dimensions	Diameter	Max. 18.4 mm
	Height	Max. 65.1 mm
Weight (Typical)		Max. 47.5 grams
Nominal Voltage		3.7 V
Internal Impedance		≤ 70 mOhm

Table4: Properties of LG18650

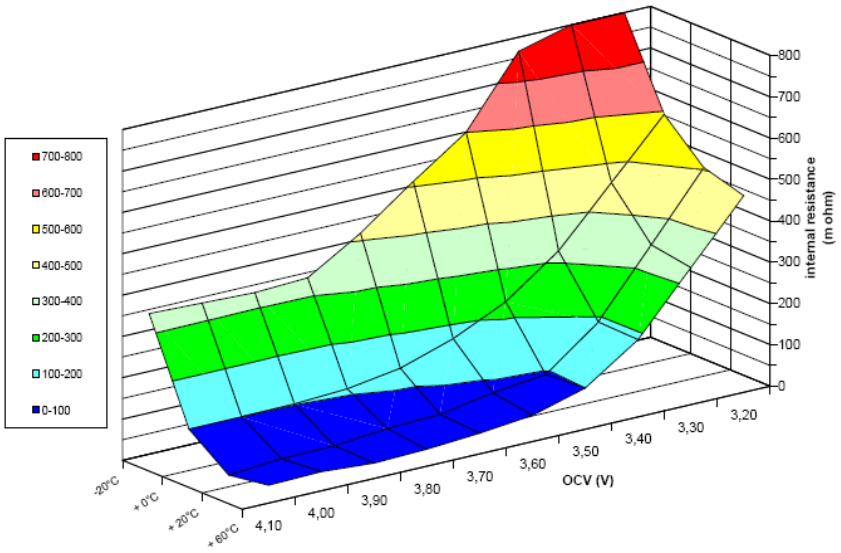

Figure 6: Battery characteristics

The variation of internal resistance of the cell with temperature and open circuit voltage is seen in the above 3-D plot. This shows the useful temperature range of the battery to lie between 0°C and 60°C. For safety purposes, it is best to operate the cells within 20°C and 40°C.

5.4 Battery charge regulation and protection

The ideal charging method for Li-ion batteries is a constant-current, constant-voltage (CCCV) charging algorithm. In this method, the battery is charged with a constant current (usually 1C) until the voltage reaches the end-of-charge (EOC) voltage. Once the EOC voltage is reached, the charger

switches to a constant voltage charging where the charging current automatically falls with time. The battery is declared “charged” when the charging current drops to a predetermined limit.

On the satellite, the maximum charging current ever available is much smaller than 1C. Also, the varying sunlight intensity makes it impossible to maintain the CCCV algorithm always. Hence, it was decided not to use any dedicated battery charger IC but to use a combination of the microcontroller and the battery protection IC for regulating the battery charging.

Battery protection ICs from Texas Instruments and Seiko Instruments were considered for the satellite. All these ICs incorporate overcharge, over discharge and overcurrent protection for two Li-ion or Li-polymer cells with the use of series FETs to allow and prevent the connection of the battery with the battery bus. The UCC3911-x (x = 1,2,3,4) from TI has internal FETs and has been used by AAUSAT before. The IC has overvoltage protection thresholds which are suitable for Li-ion cells with an EOC voltage of 4.2V. The ICs from Seiko have a large range of overvoltage thresholds and some ICs are found suitable for our battery. However, these ICs require external MOSFETs and their performance in space is unknown. The UCC3911 also provides status outputs like undervoltage, overvoltage and low power warning and also an enable pin which make them easier to work with than the Seiko products.

The specifications for UCC3911-x are:

- Protects Sensitive Lithium-Ion and Lithium-Polymer cells from overcharging and overdischarging
- Used for two-cell battery packs
- No external FETs required
- Provides protection against battery pack
- Output short circuit
- Extremely low power drain on batteries of about 20 μA
- Low internal FET switch voltage drop
- User controllable delay for tripping short-circuit current protector
- 3-A Current Capacity

state transition threshold

PARAMETER			TEST CONDITIONS	MIN	TYP	MAX	UNITS
V_{OV}	Overvoltage threshold	UCC3911–1		4.15	4.20	4.25	V
V_{OVR}	Overvoltage threshold recovery			3.60	3.70	3.80	
V_{OV}	Overvoltage threshold	UCC3911–2		4.20	4.25	4.30	
V_{OVR}	Overvoltage threshold recovery			3.65	3.75	3.85	
V_{OV}	Overvoltage threshold	UCC3911–3		4.25	4.30	4.35	
V_{OVR}	Overvoltage threshold recovery			3.70	3.80	3.90	
V_{OV}	Overvoltage threshold	UCC3911–4		4.30	4.35	4.40	
V_{OVR}	Overvoltage threshold recovery			3.75	3.85	3.95	
V_{UV}	Undervoltage threshold			2.42	2.50	2.58	
V_{UVR}	Undervoltage threshold recovery			2.90	3.00	3.10	

Table5: Threshold values UCC3911

The battery protection IC can take care of all the fault cases independent of the microcontroller. However, the microcontroller will be informed about the fault condition if detected by UCC3911-1.

5.5 Battery Box

Battery box will be a simple casing for battery. It will have FR4 like material on which batteries will be placed. Electrical connections from batteries will be taken to this PCB where the required routing will be done and connectors will be made available for further circuitry. Batteries will then be covered be exactly fitting aluminum structure with provision for temperature sensor and battery heater. The aluminum structure will be fixed to FR4 plate by screws.

Following figures gives an idea of the design.

5.6 Voltage regulators

The voltage regulator (also known as the power conditioning module) converts the raw battery or solar panel voltage into a regulated voltage for the loads. An industrial grade DC- DC converter will be used considering following factors:

1) Output voltage(s) : 3.3V, 5V
2) Input voltage range : 5-10 Volts
3) Typical and maximum output current
4) Switching frequency
5) Efficiency (>85%)
6) Output ripple
7) Electromagnetic interference(EMI)
8) Phase margin (stability)
9) Transient response
10) Soft start

11) Standby mode
12) Redundancy

The PTH08080 step-down switching regulator from Texas Instruments has been selected for this purpose. Two such modules will be paralleled together with cold redundancy.
PTR08060 was also considered. It has superior electrical characteristics, but it was discarded as it was not mechanically rugged.

The PTH08080 has the specifications:

- Up to 2.25-A Output Current at 85°C
- 4.5-V to 18-V Input Voltage Range
- Wide-Output Voltage Adjust (0.9 V to 5.5 V)
- Efficiencies Up To 93%
- On/Off Inhibit
- Undervoltage Lockout (UVLO)
- Output Overcurrent Protection (Nonlatching, Auto-Reset)
- Overtemperature Protection
- Ambient Temperature Range: –40°C to 85°C

The current limits of the modules leave a wide margin with no loss in efficiency. The wide input voltage range covers the entire useful battery voltage range of 6V to 8.4V.The modules can be switched on and off by the power systems microcontroller through the ON/OFF inhibit pin. The industrial temperature range makes the module suitable for our application.

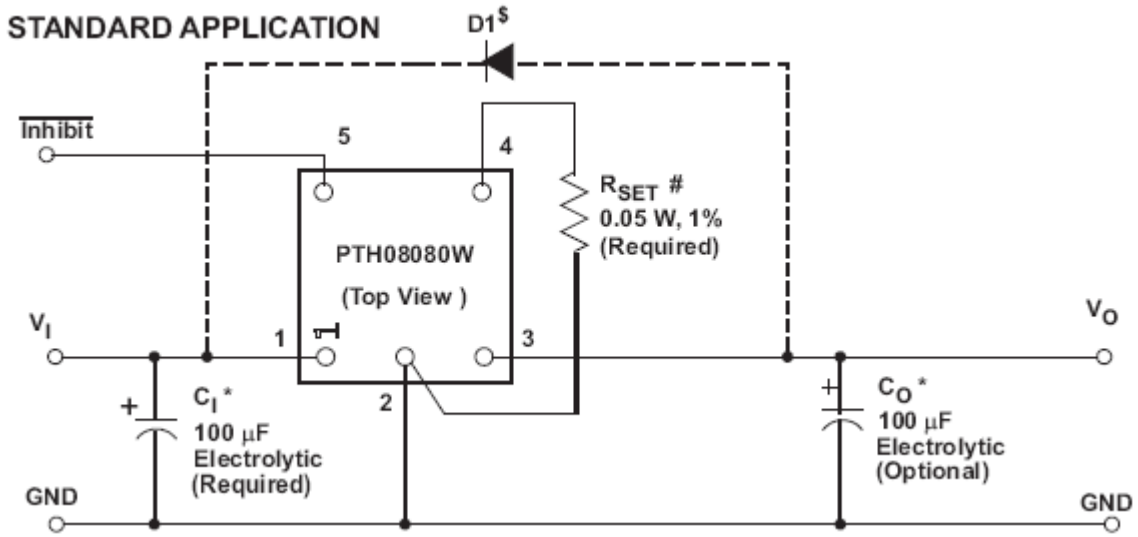

Courtesy: Texas Instruments

TYPICAL CHARACTERISTICS (12-V INPUT)[1][2]

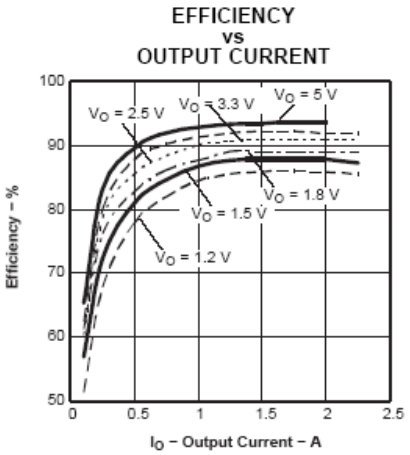

Figure 6.

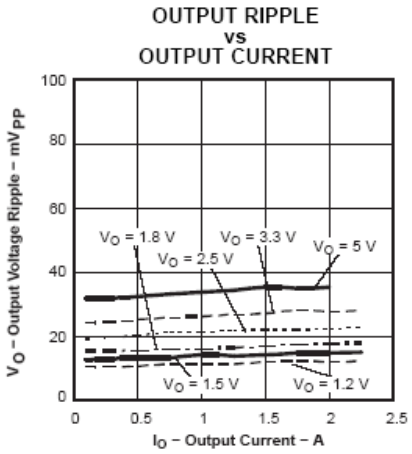

Figure 7.

Courtesy: Texas Instruments

Aluminum electrolytic capacitors cannot be used at the input and the output as they are not recommended for use below 0^{o}C. Hence, other type of capacitors like OS-CON, poly-aluminum or polymer-tantalum capacitors will be used as recommended in the datasheet. Tantalum capacitors which were used in the prototype circuit, were found to have very low reliability. Hence, CWR06 are chosen for further use. The output voltage is set by the R_{SET} resistor. A 432Ω gives an output voltage of 3.327V.

5.7 Current Distribution switches

MOSFET switches of very low internal resistance will be used for power distribution. Considering internal resistance, current capacity & flight heritage, IC tps203x from Texas Instruments was chosen. It has the following features:

- 33-mΩ internal resistance
- Ambient Temperature Range, –40°C to 85°C
- Short-Circuit and Thermal Protection ·
- Overcurrent Logic Output
- Operating Range: 2.7 V to 5.5 V
- Logic-Level Enable Input
- Typical Rise Time: 6.1 ms
- Undervoltage Lockout
- Maximum Standby Supply Current: 10 µA
- No Drain-Source Back-Gate Diode

5.8 Microcontroller

The main functions of the microcontroller are as follows:

- The microcontroller turns on the other circuits a specified amount of time after ejection from the launch vehicle.
- It regulates the charging of the battery.

- It monitors the load status information (normal/overcurrent) provided by the current limiting switches.
- Faulted loads are immediately switched off and OBC is notified.
- Voltage regulators can also be switched off in case of faults and power down.
- Faulted loads are switched ON on periodical command from the OBC.
- Readings for health monitoring are conveyed to the OBC every minute.
- Power microcontroller is powered off the battery bus by a separate linear power supply.

Since using space grade microcontrollers is prohibitively expensive, commercial ones with one-time programmable (OTP) memory will be used. An 8-bit PIC microcontroller has been chosen considering its use in various satellites like Rincosat, Stensat-2 and AAUSAT previously.

A corresponding pin compatible flash memory PIC device for the OTP device will be used to test and build all the circuits. Finally the flash device will be replaced by the OTP device. The PIC16C77 has been chosen as the flight microcontroller for the power system. The testing will be done on a PIC16F877A. The PIC16C77 has the following features:

Microcontroller Core Features:

- High-performance RISC CPU
- Only 35 single word instructions to learn
- All single cycle instructions except for program branches which are two cycle
- Operating speed: DC - 20 MHz clock input DC - 200 ns instruction cycle
- Up to 8K x 14 words of Program Memory, up to 368 x 8 bytes of Data Memory (RAM)
- Interrupt capability
- Eight level deep hardware stack
- Direct, indirect, and relative addressing modes
- Power-on Reset (POR)
- Power-up Timer (PWRT) and Oscillator Start-up Timer (OST)
- Watchdog Timer (WDT) with its own on-chip RC oscillator for reliable operation
- Programmable code-protection
- Power saving SLEEP mode
- Selectable oscillator options
- Low-power, high-speed CMOS EPROM technology
- Fully static design

Program Memory (EPROM) x 14	8K
Data Memory (Bytes) x 8	368
I/O Pins	33
Parallel Slave Port	Yes
Capture/Compare/PWM Modules	2
Timer Modules	3
A/D Channels	8
Serial Communication	SPI/I^2C, USART
In-Circuit Serial Programming	Yes
Brown-out Reset	Yes
Interrupt Sources	12

Figure 7: PIC16F877A features

PIC16f877a has some compatibility issues with the third party programmer we are using, but other microcontrollers of the same family: PIC16F84A and PIC16F628A have been tested. A universal programmer from HI-LO Systems was used for programming the PIC microcontrollers. The programs were written in assembly and compiled using the MPLAB Assembler and Simulator from Microchip. A software called WACCESS transferring the hex files to the microcontroller using the programming hardware.

The PIC16f84a and PIC16f628a were successfully programmed and tested with various codes. The following codes were simulated and tested:

- Timers using software and hardware
- Codes for testing the Low voltage programming (LVP) and High voltage programming (HVP) options. The performance of PIC16f628a with LVP was not satisfactory and PIC16f84a has only HVP.
- Codes involving ADCs were simulated but could not be tested. Neither 16F84a nor 16F628A has ADC facility.

The PIC16f877a was found to have a problem with the system clock. As the same issue was observed on three ICs, there might be some problem with the configuration bit settings set by the programmer.**(***reference: Design with PICMicrocontrollers, John B.Peatman, Pearson Education, page no 9).*Now we have decided to buy a PIC programmer available from Microchip itself.

We have the radiation testing data for the PIC16f877a device. And the corresponding OTP device has similar architecture. This data will be useful as we might not be able to do any actual radiation testing on the devices we have.

5.9 Hardware list

Sr. no.	Component	Description	Nos. used
1.	Solar cells	GaAs 18% eff. , 0.87V V_{MP}	52
2.	Batteries	SAFT 3.7V, 5.8Ah	4
3.	3.3V regulator	TI PTR08060, integrated switch-mode regulator	2
4.	5V regulator	TI PTH08080, integrated switch-mode regulator	2
5.	Microcontroller	Microchip PIC16C77	1
6.	Power distribution	TI TPS203x, current limiting switches	5
7.	Battery protection	UCC3911-1	2
8.	Power OR-ing diodes	MBRS320	4
9.	RBF pin, kill and charging switches	TBD	

Table 6: List of Hardware

6. Software

Software for micro-controller is written in Assembly language. A basic framework for the final code has been written and tested. Micro-controller monitors five loads and communicates with On board

computer with SPI interface. This protocol was tested and working with corresponding families of micro-controller. Over-current is detected by five current limiting switches. The micro-controller switches off that load and notes it. Also, two critical currents and three critical voltages are read and saved. Currently, it can accept command through UART. Accordingly, command is executed and critical quantities and load status data is sent back

Flowchart for the code is attached separately due to formatting issues.

Following work is to be done in software development.

1. Prelaunch tests and debugging
2. Start-up
3. Various failure scenarios and their mitigation
4. Use of data encoding

Study was done to check the requirement and feasibility of error detection and correction. After a review, it was decided not to have any encoding.

7. Health Monitoring:

The Battery Protection IC UCC3911-1 gives Overvoltage, undervoltage and Low Power warnings. The Overvoltage and Low Power warning for both the ICs will be monitored by Power microcontroller and the status will be conveyed to OBC microcontroller.

The power circuit has five Current limiting switches (tps203x) which supply to various loads. In case the current exceeds the maximum limit, the IC gives an OC output which will also be monitored and the observations will be sent to OBC microcontroller periodically.

Tentative frequency for this monitoring is once a minute.

8. Safe Mode:

This mode shall be entered when the power drops below a threshold.

The components will be switched off in the following manner, by the Power circuit:

- monopole 2
- All control sensors and magnetorquer
- OBC circuit
- Beacon
- Power circuit

The value of the threshold is to be decided.

9. Reliability Analysis of Power sub-system

Infant mortality rate and MTBF of Power system are calculated independently. Reliability values of standard components were taken from datasheets if mentioned. Else values form Military standard MIL-STD-217F were used. Failure of any one component implies failure of the system.

Power circuitry has incorporated redundancy wherever the reliability was found to be low. Two of the four DC-DC converters are redundant. A spare battery and battery protection circuit is used. This has led to high reliability of power system.

In case redundant component is used, failure of both components implies failure of the system. For solar panels, failure of 2 or more panels was considered as failure.

Infant mortality rate was found to be 700ppm or 0.07%.

Reliability of the complete power system was calculated to be 0.9977

Appendices:

Power Budget:

Circuit	Voltage	Avg. Current	Peak Current	Avg. power	Peak power
	(V)	(A)	(A)	(W)	(W)
Beacon	3.3	0.22	0.22	0.750	0.750
	3.3	0.055	0.22	0.187	0.750
Downlink	3.3	0.7	0.7	0.083	2.400
GPS	5	0.6	0.6	0.375	2.500
Sun Sensors	5	0.01	0.01	0.050	0.050
Magnetometer	7.4	0.03	0.03	0.222	0.222
Magneto-torquer	5	0.1035	1.035	0.518	5.175
Torquer driver	5	0.00325	0.0325	0.016	0.163
OBC	5	0.2	0.3	1.500	1.500
Battery Heater	7.4	0.5	0.5	0.300	3.700
Total				3.251	16.346

Including losses in power system, the average power requirement goes to 4.3Watts.

Power Requirement in worst case eclipse

Time over India = 1000sec
Time over ground station = 500sec

Circuit	Voltage	Avg. Current	Peak Current	Avg. power	Peak power
	(V)	(A)	(A)	(W)	(W)
Beacon	3.3	0.21	0.21	1.584	1.584
	3	0.05	0.21	0.462	1.584
Downlink	3.3	0.55	0.55	4.092	4.092
GPS	5	0.4	0.4	2.000	2.000
Gyroscopes	5	0.004	0.004	0.018	0.018
Sun Sensors	5	0.01	0.01	0.050	0.050
Magnetometer	8	0.03	0.03	0.240	0.240
Magneto-torquer	5	0.104	1.035	0.518	5.175
Torquer driver	5	0.003	0.033	0.016	0.163
OBC	3.3	0.3	0.3	0.990	0.990
Battery Heater	8	0.5	0.5	4.000	4.000
	0	0	0	0.000	0.000
Total				7.831	19.895

Battery bus	8	2.35
3.3V bus	3.3	1.86
5V bus	5	0.50

This adds up to 5Watt-hrs.

Considering losses in Power system, total power delivered by battery ~6.5 Watt-hrs.

Battery Charge Simulation Results:

Battery undergoes cycling of charge condition dominated by following two factors:

1. Solar power, which periodically falls to zero for around 33 minutes in each orbit during eclipse period.
2. Battery protection IC does not let the battery charge when battery is in Over Voltage state. Overvoltage state is the condition when battery voltage is falling from 4.2 to 3.7.
3. Communication load is active for few minutes in some of the orbits. This has a small impact on battery charge.

Simulations have produced results as shown

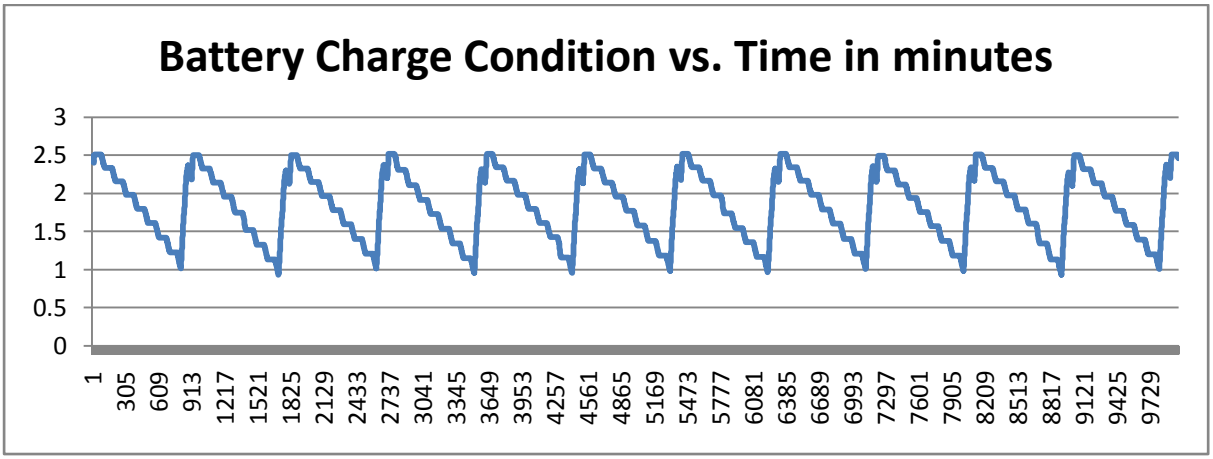

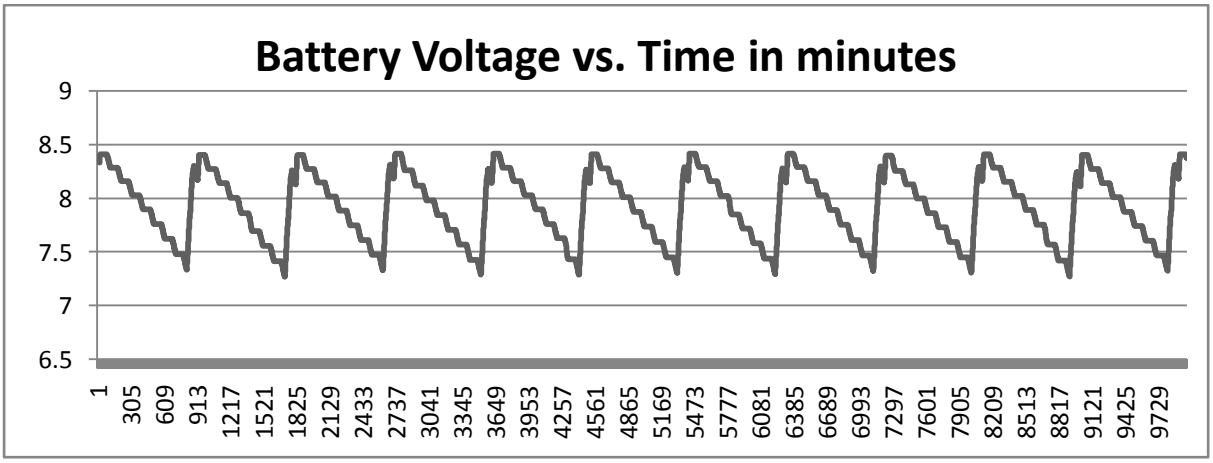

So, we can consider that the battery undergoes 600 cycles of 60% DOD. This DOD is much higher that required by other sub-systems, mainly due to battery protection IC which is not suitable.

The DOD can be significantly reduced if some other technique of battery protection is used.

A comparative study for the same is being done, to reconsider the options that were rejected earlier.

Power generated on the satellite due to Earth Albedo

Earth Albedo

The sunlight reflected off the Earth's surface is called “Albedo” or “earth Albedo” and it is conventionally measured as a fraction of the direct incident sunlight. The Earth albedo induces power in solar cells just like direct sunlight. The Earth albedo model presented here (by D.N.Bhanderi , Alborg university, www.bhanderi.dk) , calculates the amount of Earth albedo arriving at an object in space, maintaining information of direction of the Earth albedo, useful for objects in low Earth-orbit. The directional information is maintained by partitioning the Earth surface in small cells, and calculating the Earth albedo contribution of each cell, rather than assuming a total amount from the nadir direction.

Input Data:

In order to calculate the Earth albedo, the model needs three input parameters in the ECEF (earth centred earth fixed) frame:
Satellite position vector, Sun position vector, Earth surface reflectivity.
The partitioning is defined by the resolution of the input reflectivity data. Reflectivity data is available from the total ozone mapping spectrometer (TOMS) project ,NASA (http://toms.gsfc.nasa.gov/reflect). Matlab converted data and pre-processed data are available within the Earth Albedo Toolbox, which also includes Matlab functions for loading TOMS data into Matlab manually. The resolution of the TOMS data is 180 x 288 data points.
That is 51,840 cells of 1 deg latitude and 1.25 deg longitude. This resolution may be decreased in the toolbox software.
Figure 1 below shows the plot of the 2004 annual mean of the TOMS reflectivity data as a percentage of the direct solar radiation intensity (=1376 W/m^2).

Fig 1 : 2004 annual mean reflectivity

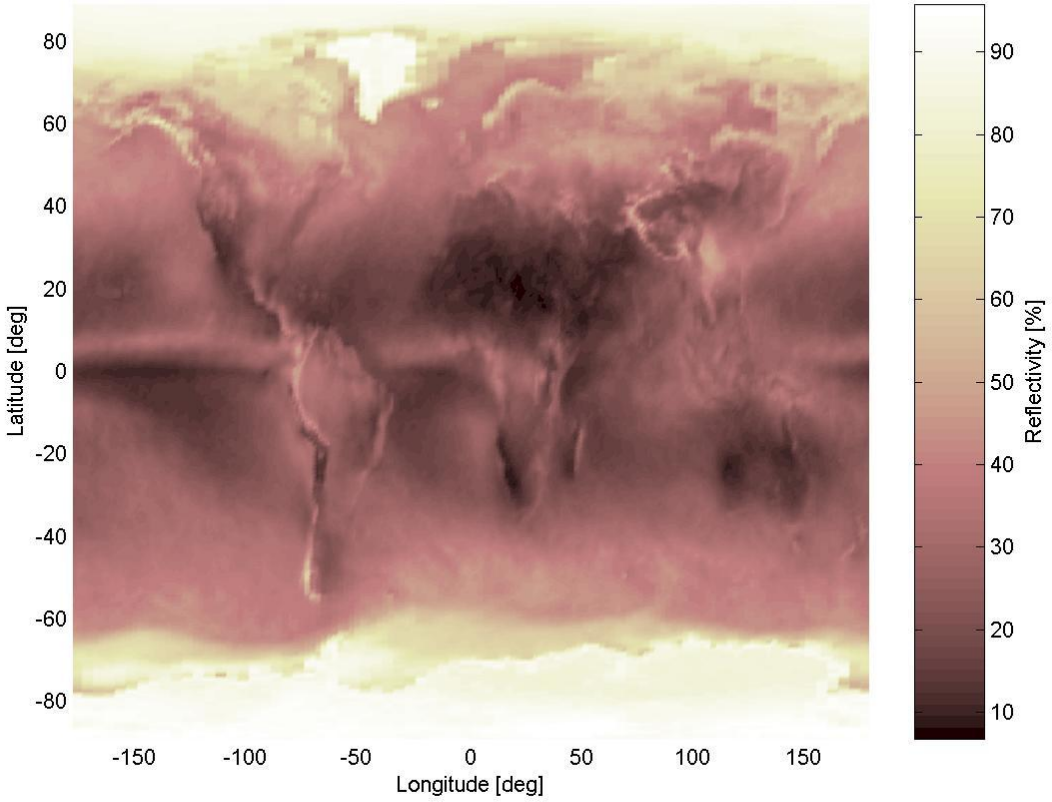

Mathematical Model (the MATLAB toolbox):

The model calculates the Earth albedo from each data point in the reflectivity data. The simplified reflection model is shown in Figure 3. The grid point (θ, ϕ) defines the longitude and lattitude of the data point. This point defines a cell with an area A(ϕ) expanded by 1 deg latttitude and 1.25 deg longitude. The incident irradiance E_0 arrives from the direction $\hat{r}_{sun}$ to the Sun , the angle of which is defined from the cell normal $\hat{n}_c$. The incident irradiance is assumed to be constant for all cells. The direction of the satellite is defined by $\hat{r}_{sat}$, also defined by an angle to the cell normal. The reflected irradiance at satellite distance from the cell centre is denoted $E_c(\theta, \phi)$.
Figure 2 below shows all these parameters.

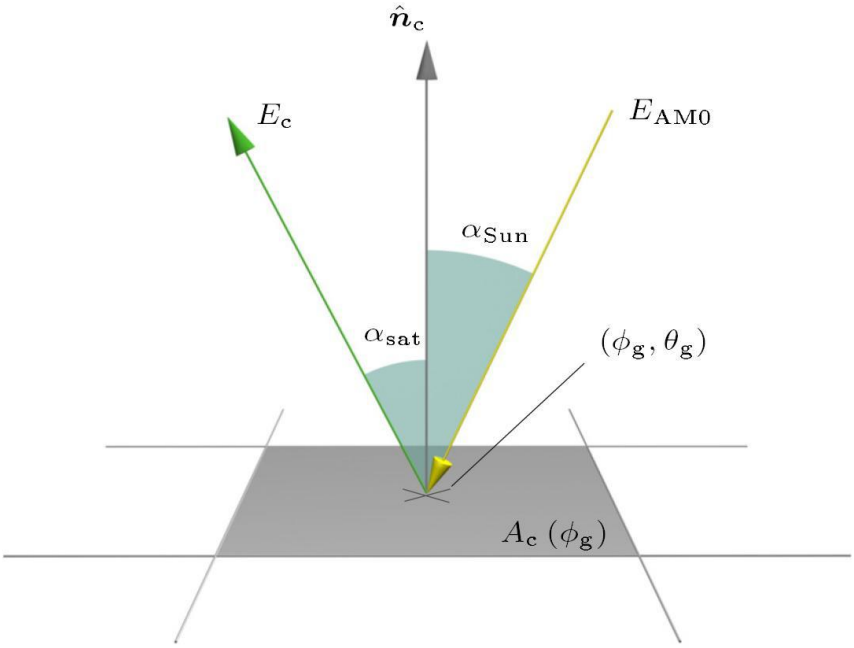

Fig 2 : Cell parameters

$\rho(\theta, \phi)$ is the mean reflectivity of the cell as obtained from the database, ehich contains per-cell reflectivity for each day of the years 2000-2005 (we are currently using the data for a fixed date only) .

Given the above definitions, a matrix of contributions from each cell in the input data is calculated.

$$E_c(\theta, \phi) = \frac{\rho(\theta, \phi) E_0 A(\phi)(\hat{r}_{sun} \,.\, \hat{n}_c)(\hat{r}_{sat} . \hat{n}_c)}{\pi |\hat{r}_{sat}|^2} \quad \text{for cells which are sunlit}$$

$$= 0 \qquad \text{otherwise}$$

However, unlike the incident irradiance , this irradiance is not uni-directional. When calculating the output of photo voltaics, higher accuracy is achieved by calculating the contribution to the power output from each cell, and incorporating the direction to each cell in the calculations. This is done using the perpendicular equivalent Simulink block.

using the following equation, assuming simple cosine dependency on output current and angle of incidence, where is the measured output on the photo voltaics, is the output current measured, when illuminated with an irradiance of , and is the direction to the grid point (or cell center). The angle of incidence is measured relative to the normal to the photo voltaic plane.

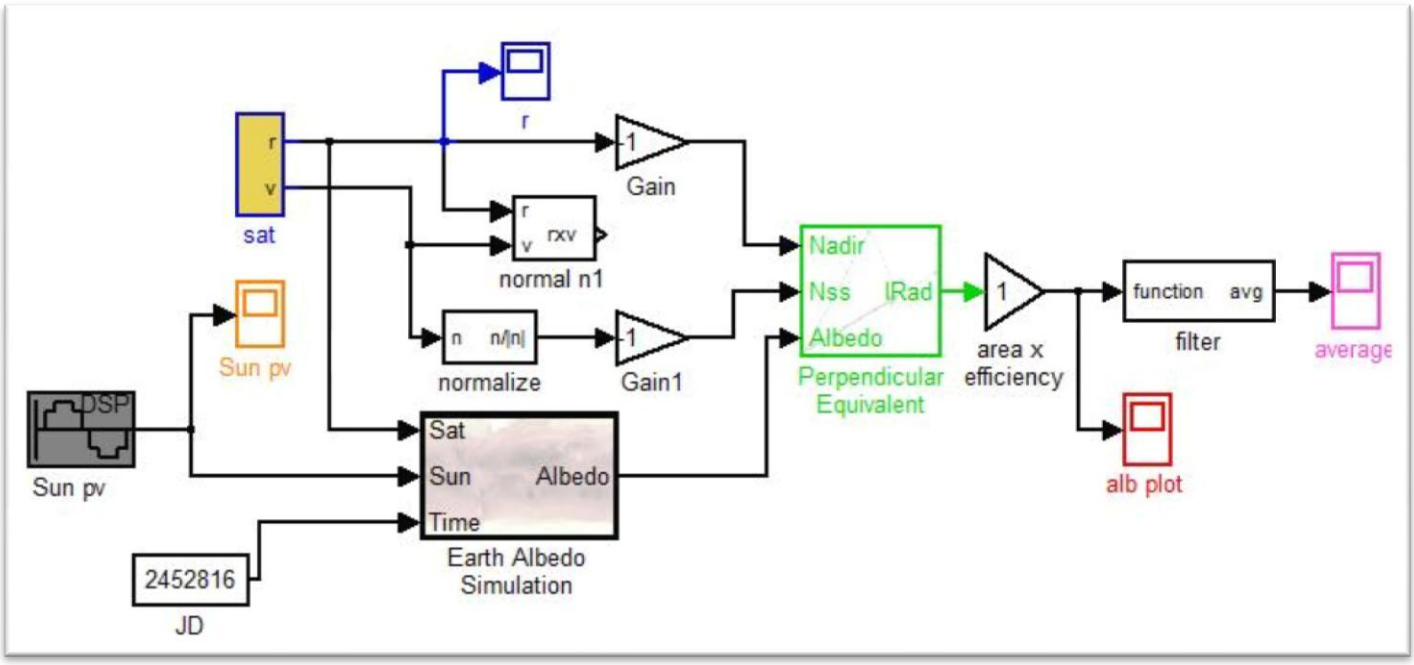

Fig 3: The Simulink Model

Description of the simulink model:
The 'earth albedo simulation' and 'perpendicular equivalent' are the main blocks which calculate the albedo, using previous year's reflectivity data given the position of the satellite and the sun in the ECEF frame. This frame is shown in figure 4. The reflectivity data is taken for the day indicated by the bottom left block ,the Julian Date. The JD 2452816 in the figure corresponds to 25th of June, 2003.
The grey block on the bottom left gives the sun's co-ordinates in the same frame ,this is simply $x = 1.5\ AU \sin \omega t$, $y = 0, z = 1.5\ AU \cos \omega t$. We have neglected the earth's revolution ; i.e. the sun's motion is taken to be in a fixed plane. This is justified since the satellite's life is of the order of 4 months and we are looking only at daily, not annual variations. The yellow block "sat" gives the satellites position and velocity vectors.

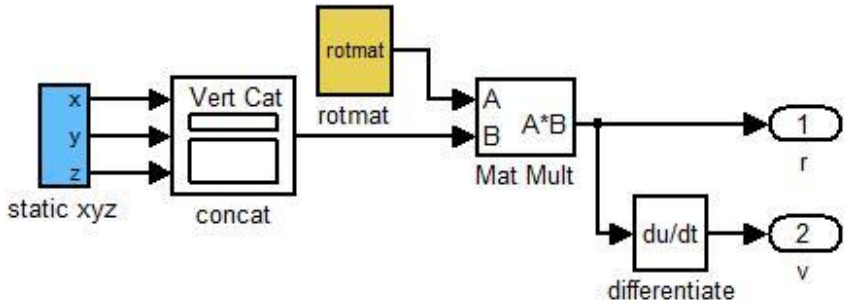

Fig 4: construction of the "sat" block

The 'static xyz' block gives the position in an Earth centred (but not fixed) frame as below.

$$\vec{r}(t) = R\begin{bmatrix} \cos\lambda & \sin\lambda & 0 \\ -\sin\lambda & \cos\lambda & 0 \\ 0 & 0 & 1 \end{bmatrix}\begin{bmatrix} \sin(\omega t) \\ \cos(\omega t)\sin 8° \\ \cos(\omega t)\cos 8° \end{bmatrix} = R\begin{bmatrix} \cos\lambda\sin(\omega t)+\sin\lambda\cos(\omega t)\sin 8° \\ -\sin\lambda\sin(\omega t)+\cos\lambda\cos(\omega t)\sin 8° \\ \cos(\omega t)\cos 8° \end{bmatrix}$$

Here $\lambda = 22.5^0$ and $R = 7070\ km$ are orbit parameters.

This is multiplied by the corresponding y-rotation matrix (rotmat) to obtain the position in the ECEF frame, which on differentiation yields the velocity.

$$rotmat = \begin{pmatrix} \cos\omega t & 0 & \sin\omega t \\ 0 & 1 & 0 \\ -\sin\omega t & 0 & \cos\omega t \end{pmatrix}$$

Fig 5: Normals to the satellite **Fig 6: the ECEF frame**

The nadir vector is simply the negative of the satellite's position vector.

The face normals (which must necessarily be unit vectors) are, for the purpose of calculation, taken to be ±v, ±(rxv) , as shown in figure 5 above.
These normals are fed through the "normal n1"

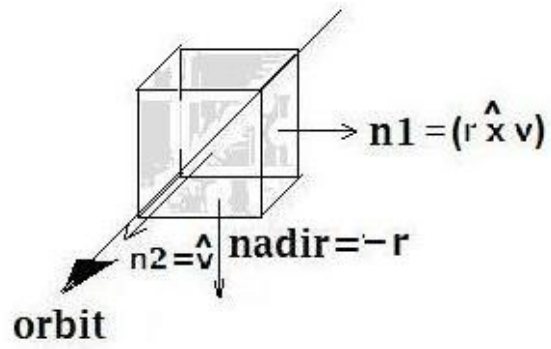

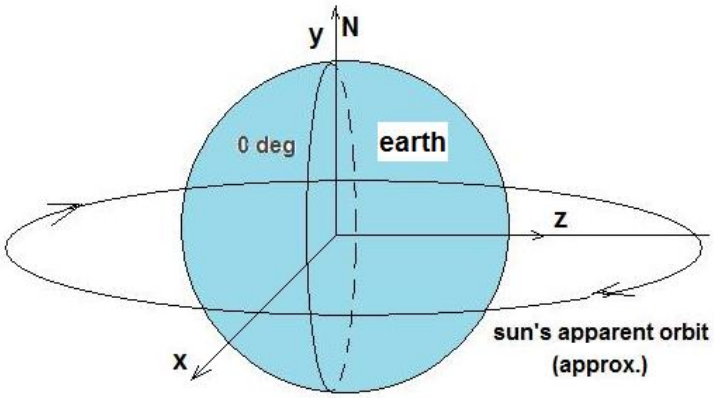

and "normalize" blocks ,one at a time. The -1
gain allows us to switch between v and –v faces, for example.

The last block computes the average as $g(f) = \int_0^t f\ dt / \int_0^t dt$.

Lastly ,the 'area x efficiency' gain was used so that we could plot directly the generated power as required (currently it is set to 1).

Note that even if assume fixed orientation of the faces we get a good approximation of the net power generated, since the sum of projections of the panel face-areas rotated at an arbitrary angle perpendicular to the radius vector is independent of the angle.

The perpendicular equivalent of the albedo(in W/m^2 on Y axis) plotted for 8.64×10^4 sec (1 day ~ 14 orbits) is shown below.

Fig 7.1: Albedo on the face n1(refer to fig 5)

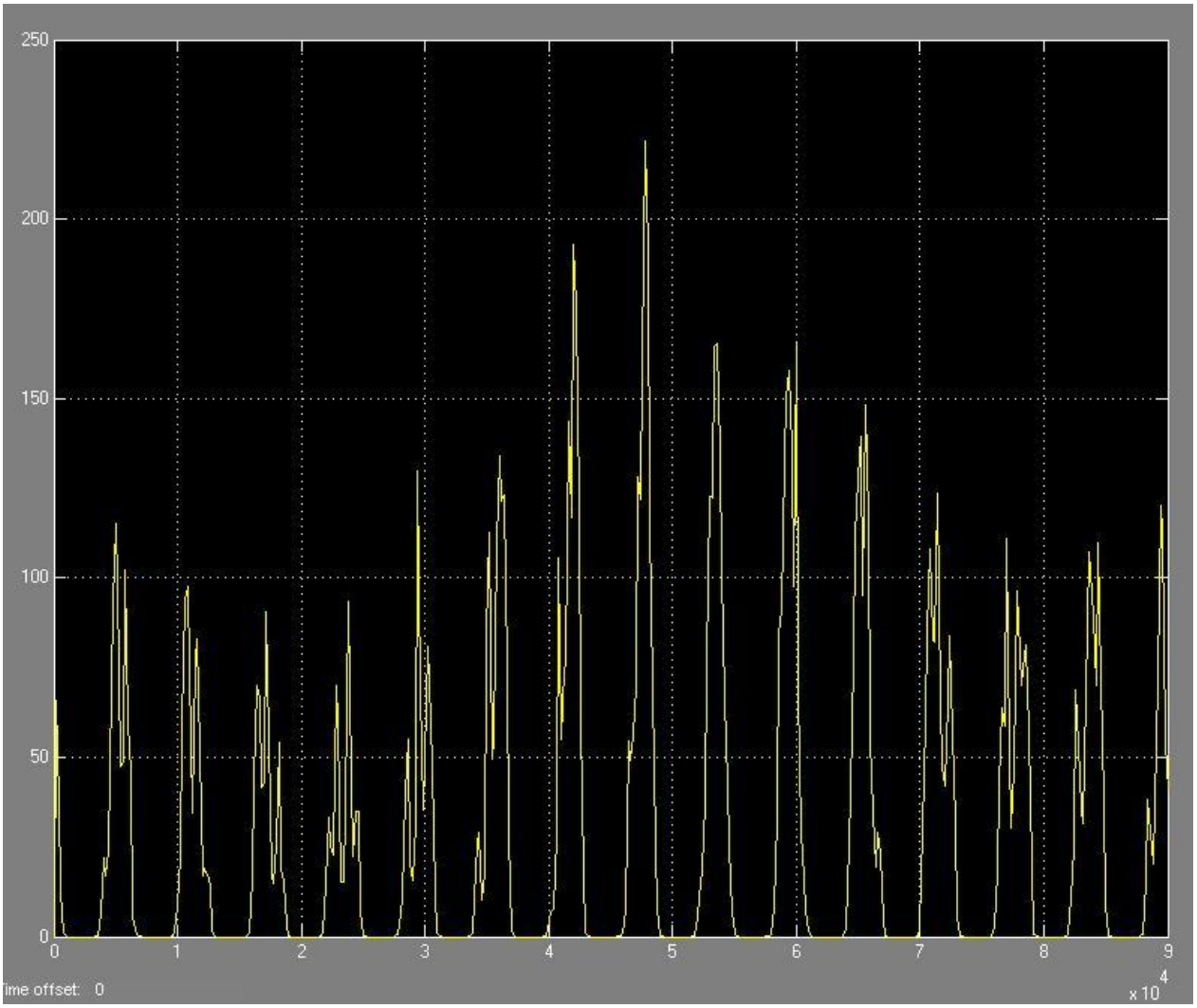

Fig 7.2: Albedo on the face –n1 (refer to fig 5)

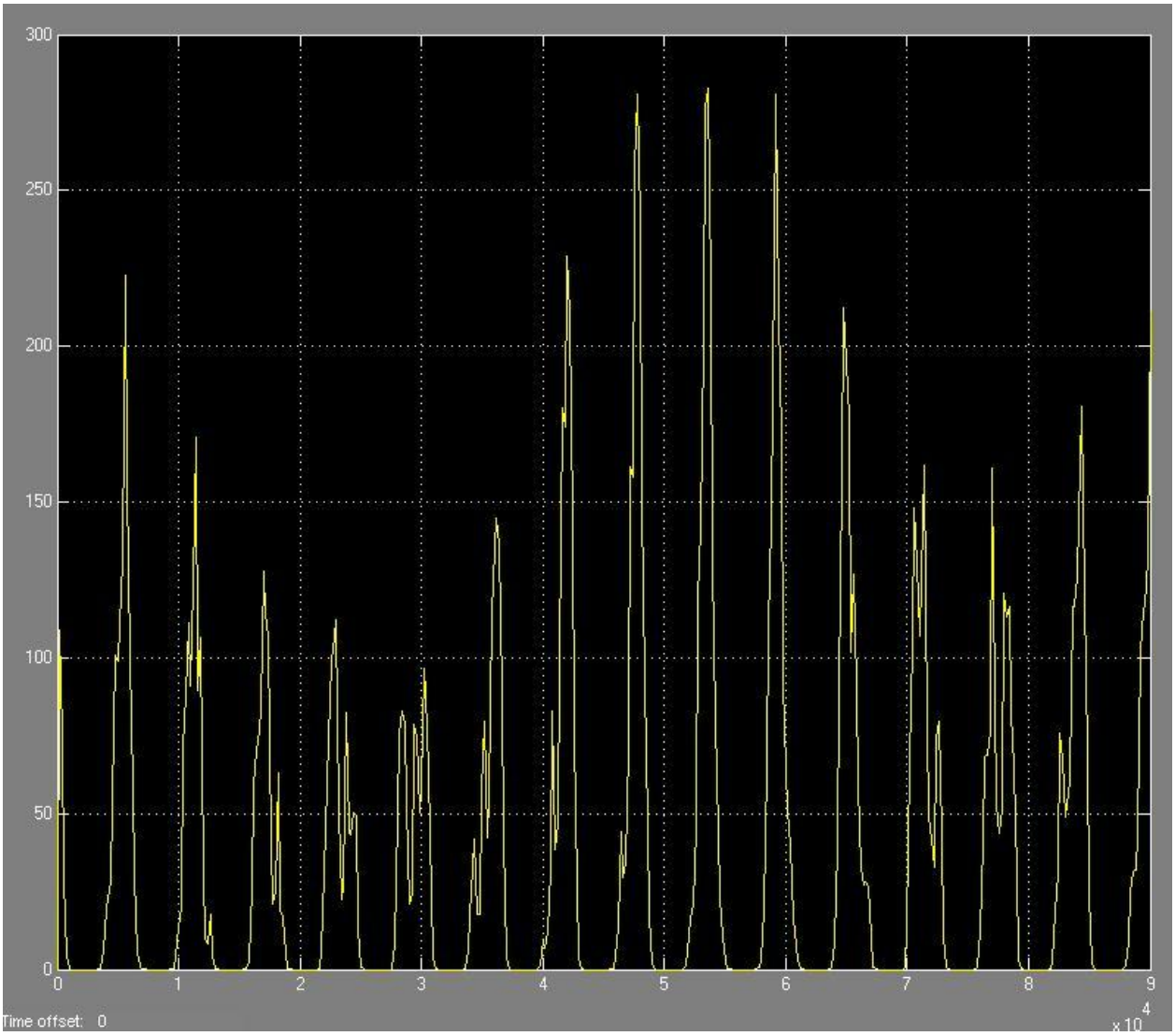

Fig 7.3: Albedo on the face n2 (refer to fig 5)

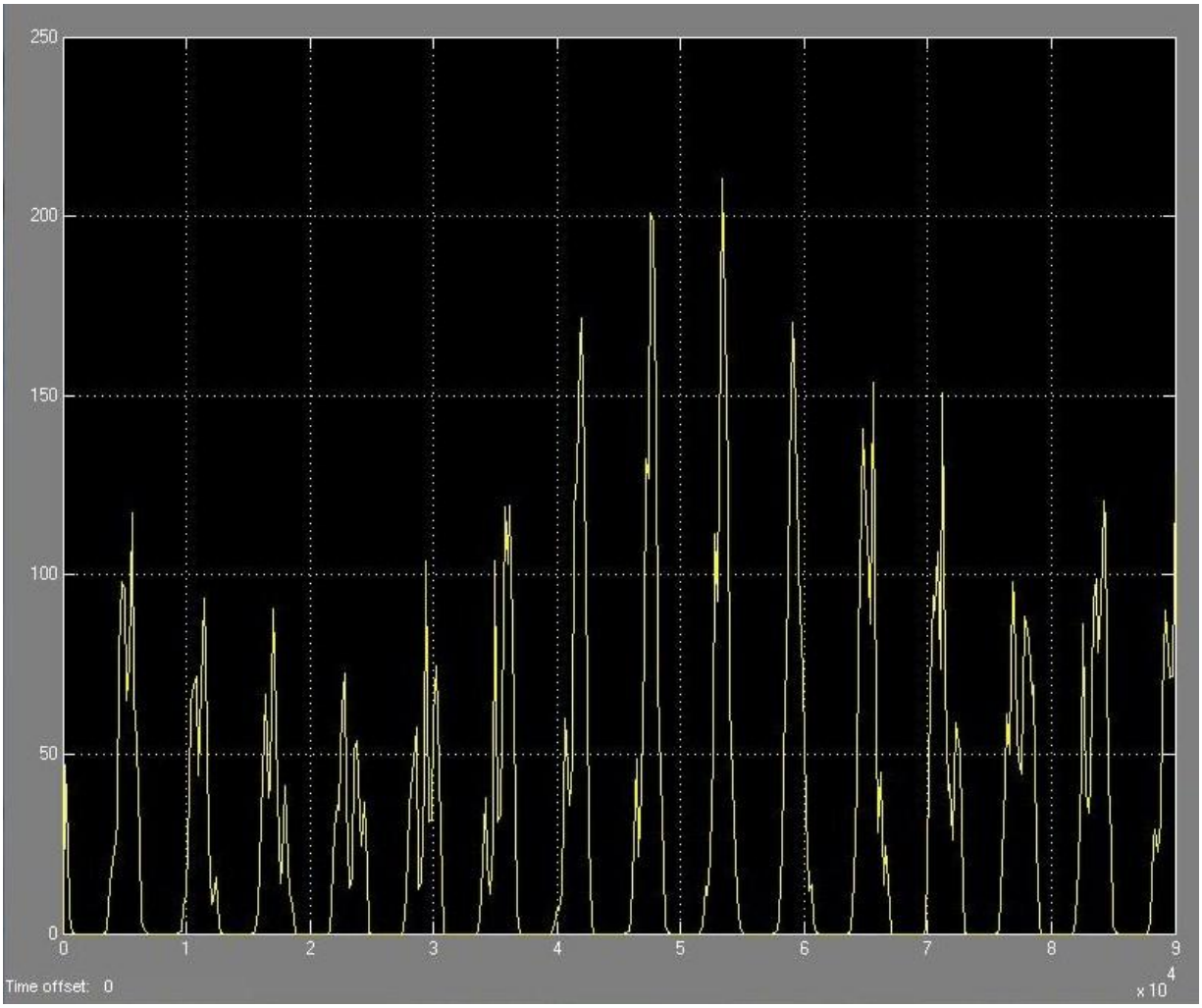

Fig 7.4: Albedo on the face –n2 (refer to fig 5)

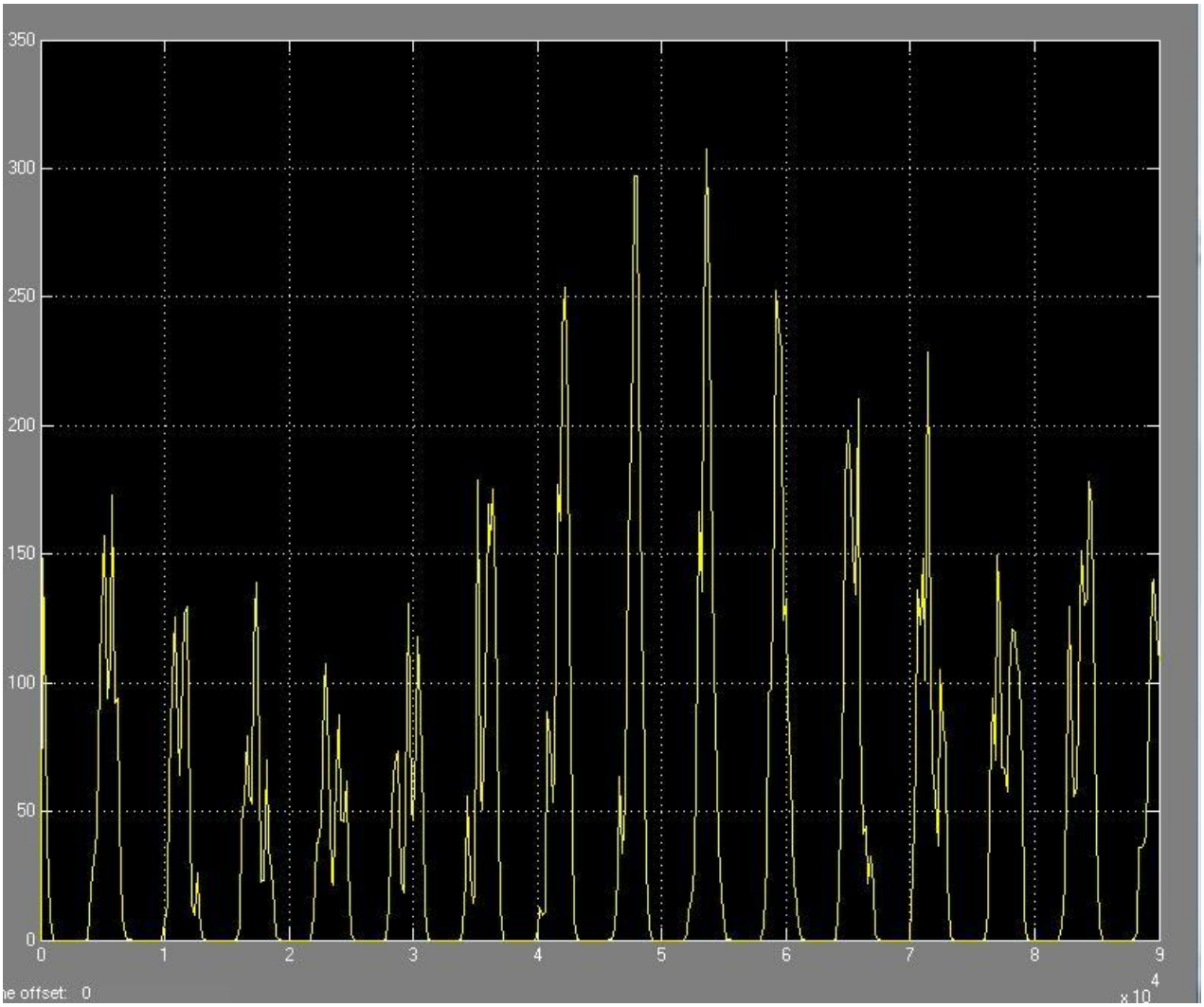

Fig 7.5: Albedo on the nadir face (refer to fig 5)

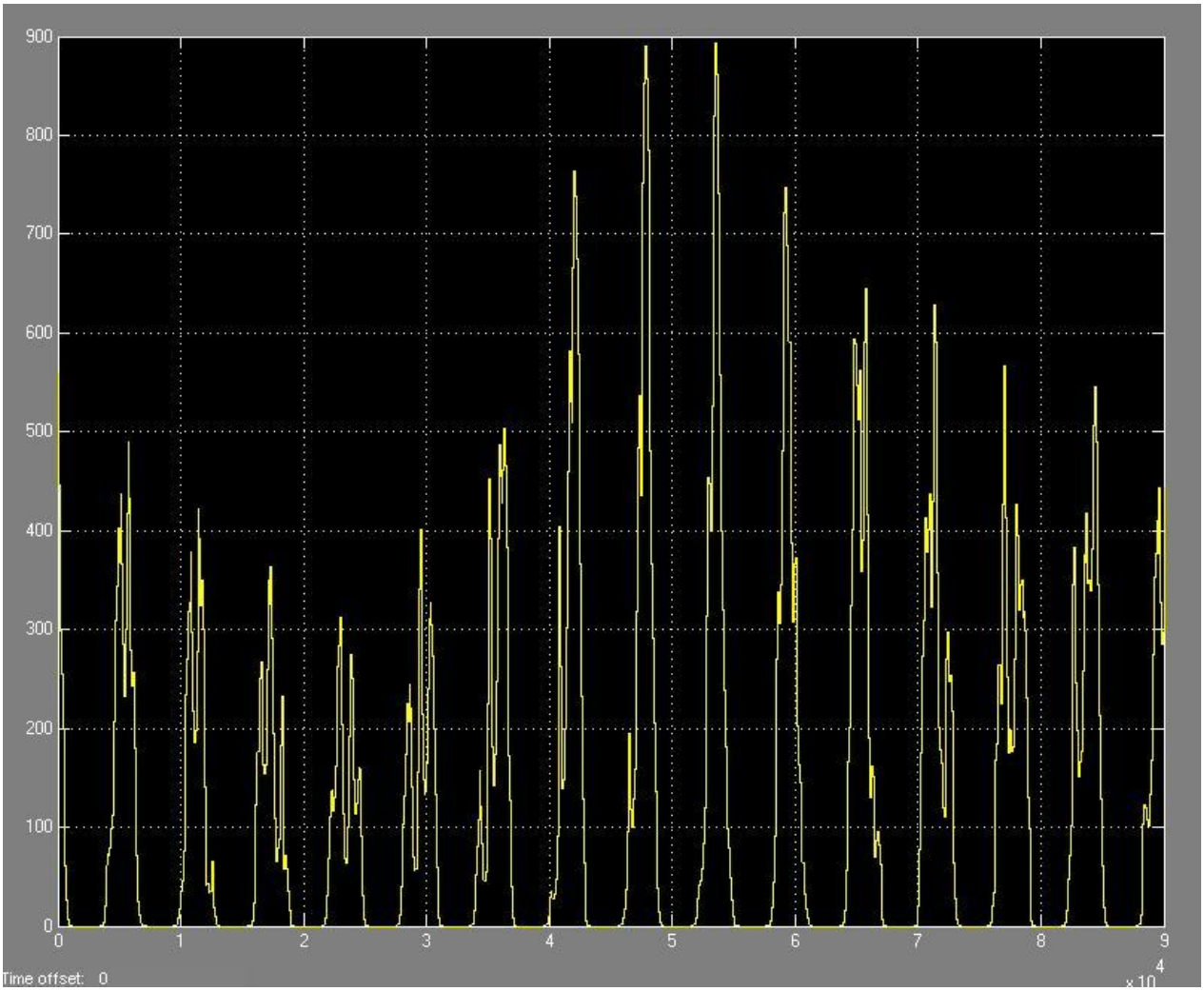

Note that though the albedo on the nadir face is the highest (as is expected) we do not consider it as there are no solar cells on the nadir face.

interest is the daily average albedo incident on each face and the power it generates. This was calculated by the last block in the model.

Face	Daily average albedo (W/m^2)
n1	40.1
-n1	29.8
n2	31.8
-n2	38.6
Total	150.3

It is of significance to note that the total average power generated due to the earth's albedo is less than 5% of the power due to solar radiation. Hence we will be neglecting the former in comparison to the latter.

Solar Power Calculations:

Direct solar radiation:

The intensity of sunlight available near Earth is about 1353 W/m^2. The actual value varies by 6.9% percent through the year but the standard accepted value of the solar constant (*S*) is 1353 W/m^2. The energy distribution of sunlight at the top of the Earth's atmosphere is called the AM0 (air-mass 0) spectrum. For the surface of the Earth, other spectrums AM1 and AM1.5 are used as standards for testing solar cells.

Sunlight reflected from the Earth: The surface of the Earth and the atmosphere reflect the incident sunlight to a significant degree. The ratio of the energy reflected diffusively to the energy incident is called albedo. The albedo of Earth is different at different places; it is close to 1 near the poles whereas it is quite small over oceans. The average value is around 30%.

Earth's thermal radiation: Earth emits light in the infrared region. The intensity of this thermal radiation is about 237 W/m^2 in a low Earth orbit (LEO).

Body mounted solar panels

The satellite is a cuboid with a size of 260mm x 260 mm x 260mm. One of the faces is required to be pointing to the Earth at all times for communication. Another face is required to be in the direction of motion of the satellite for the payload. Solar panels are present on A, B, B', C faces. Face C' does not receive solar flux for the planned orbit.

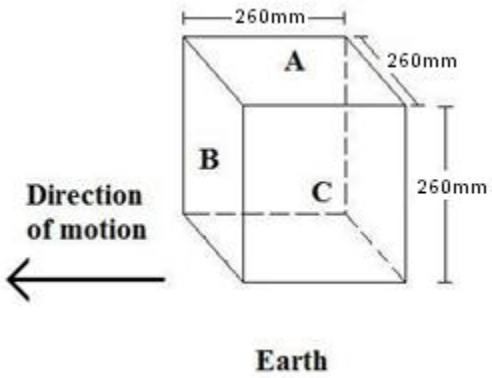

Figure 8: Satellite size

In the accompanying figure, the faces A, B and C are mutually perpendicular. The faces opposite to them are named as A',B' and C' respectively. A' is the nadir surface and A is the zenith surface. C is the sun facing side, while C' is anti sun facing. The satellite moves in the direction along the outward normal to B.

Since the antennae are oriented with a slight angle towards the Earth, they do not obstruct the path of direct sunlight falling on the solar panels. Hence, a shadow analysis is not required for the direct solar radiation.

The total useful power on each of the faces is found to be:

A	A'	B	B'	C	C'	Total
14W	1W	10W	8W	12W	0W	45W

The calculation of these numbers is detailed below.

Direct solar power calculation

The satellite is to be placed in a 10.30 am Sun-synchronous orbit with a 98° inclination at an altitude of 670 km. The radius of the satellite orbit is thus, R = 7070km. The time period of the orbit is T = 5916 sec (98.6 minutes). Hence, the satellite's angular velocity of rotation about the Earth is $\omega = 0.00106$ rad/sec.

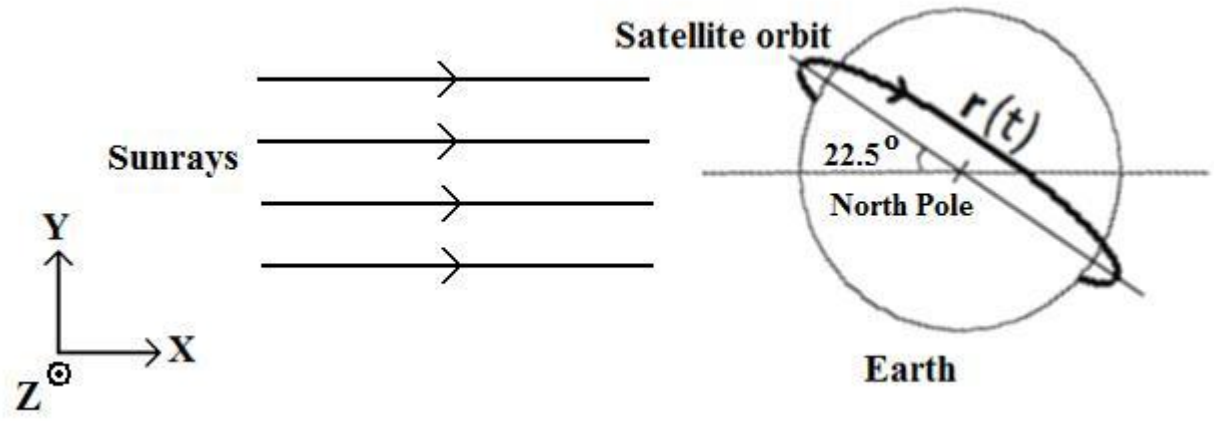

Figure 9: Satellite orbit

In the above diagram, Earth is taken as the origin for the coordinate system. The position of the satellite as a function of time, starting with the point just above the North Pole is

$$\therefore \vec{r}(t) = R\begin{bmatrix} \cos\lambda & \sin\lambda & 0 \\ -\sin\lambda & \cos\lambda & 0 \\ 0 & 0 & 1 \end{bmatrix}\begin{bmatrix} \sin(\omega t) \\ \cos(\omega t)\sin 8° \\ \cos(\omega t)\cos 8° \end{bmatrix} = R\begin{bmatrix} \cos\lambda\sin(\omega t)+\sin\lambda\cos(\omega t)\sin 8° \\ -\sin\lambda\sin(\omega t)+\cos\lambda\cos(\omega t)\sin 8° \\ \cos(\omega t)\cos 8° \end{bmatrix}$$

Hence, the velocity of the satellite is

$$\therefore \vec{v}(t) = R\omega\begin{bmatrix} \cos\lambda\cos(\omega t)-\sin\lambda\sin(\omega t)\sin 8° \\ -\sin\lambda\cos(\omega t)-\cos\lambda\sin(\omega t)\sin 8° \\ -\sin(\omega t)\cos 8° \end{bmatrix}$$

Thus, the normals to the three faces A, B and C are found to be

$$\hat{n}_1(t) = \begin{bmatrix} \cos\lambda \sin(\omega t) + \sin\lambda \cos(\omega t)\sin 8° \\ -\sin\lambda \sin(\omega t) + \cos\lambda \cos(\omega t)\sin 8° \\ \cos(\omega t)\cos 8° \end{bmatrix}$$

$$\hat{n}_2(t) = \begin{bmatrix} \cos\lambda \cos(\omega t) - \sin\lambda \sin(\omega t)\sin 8° \\ -\sin\lambda \cos(\omega t) - \cos\lambda \sin(\omega t)\sin 8° \\ -\sin(\omega t)\cos 8° \end{bmatrix}$$

$$\hat{n}_3(t) = \hat{n}_1(t) \times \hat{n}_2(t)$$

From this, the angle of incidence of sunlight on the faces A, B and C are found. If the angles are denoted as α, β and γ respectively, then

$$\cos\alpha = -\hat{i} \cdot \hat{n}_1(t) = -\cos\lambda \sin(\omega t) - \sin\lambda \cos(\omega t)\sin 8°$$

$$\cos\beta = -\hat{i} \cdot \hat{n}_2(t) = -\cos\lambda \cos(\omega t) + \sin\lambda \sin(\omega t)\sin 8°$$

$$\cos\gamma = -\hat{i} \cdot \hat{n}_3(t) = -\sin\lambda \cos 8°$$

The intensity of light incident on face A is

$$I_A = S\cos\alpha \text{ when } \cos\alpha > 0 \text{ and } 0 \text{ otherwise}$$

Similarly, for the other faces,

$$I_{A'} = S\cos\alpha \text{ when } \cos\alpha < 0 \text{ and } 0 \text{ otherwise}$$

$$I_B = S\cos\beta \text{ when } \cos\beta > 0 \text{ and } 0 \text{ otherwise}$$

$$I_{B'} = S\cos\beta \text{ when } \cos\beta < 0 \text{ and } 0 \text{ otherwise}$$

$$I_C = S\cos\gamma \text{ when } \cos\gamma > 0 \text{ and } 0 \text{ otherwise}$$

$$I_{C'} = S\cos\gamma \text{ when } \cos\gamma < 0 \text{ and } 0 \text{ otherwise}$$

The averages of I_A, $I_{A'}$, I_B, $I_{B'}$, I_C and $I_{C'}$ over one orbit have to be calculated taking the eclipse region into account.

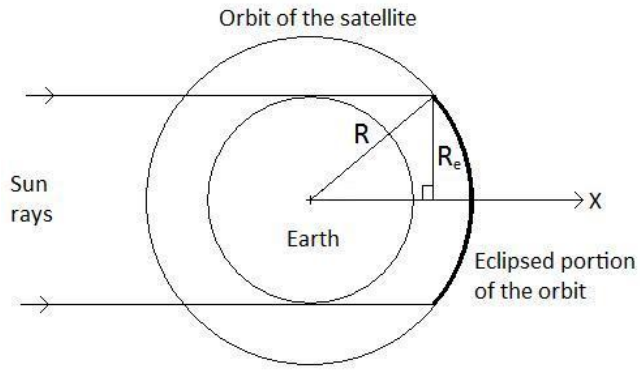

From the adjoining figure, we can see that the satellite enters the eclipsed region when,

Figure 10: The eclipsed portion of the orbit

$$x > \sqrt{R^2 - R_e^2}$$

$$\Rightarrow R(\cos\lambda \sin(\omega t) + \sin\lambda \cos(\omega t)\sin 8°) > \sqrt{R^2 - R_e^2}$$

$$\Rightarrow 0.925\sin(\omega t + 3.3°) > 0.425$$

$$\Rightarrow \sin(\omega t + 3.3°) > 0.46$$

$$\Rightarrow 27.4° < \omega t + 3.3° < 152.6°$$

$$\Rightarrow 24.1° < \omega t < 149.3°$$

The intensities I_1, I_2 and I_3 are now plotted over the period of one orbit and their averages are found.

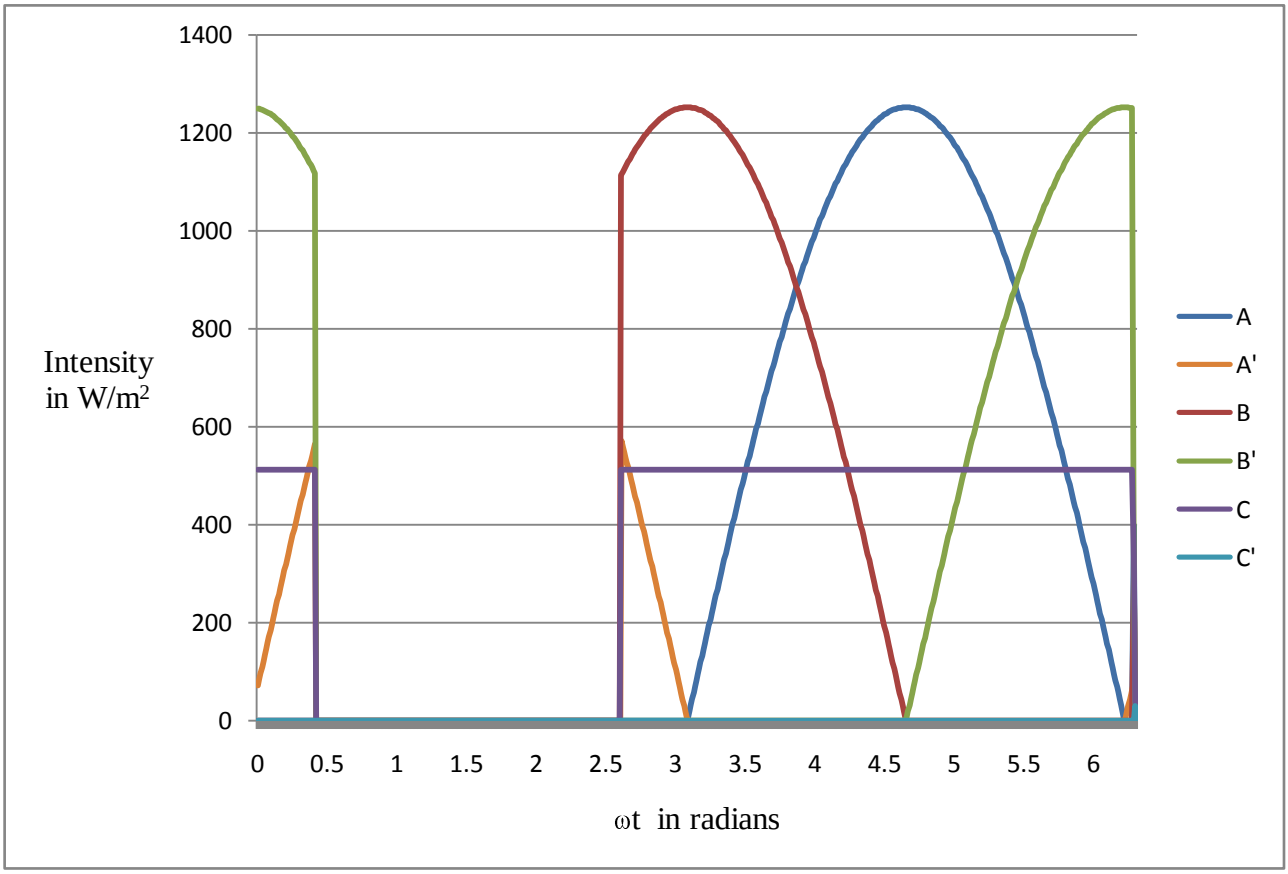

Figure 11: Direct solar intensities over the faces

The average intensities on the faces over one orbit are:

A	A’	B	B’	C	C’
398 W/m^2	44 W/m^2	291 W/m^2	291 W/m^2	334 W/m^2	0 W/m^2

Reliability Analysis: Nominal Mode

Component	Base MTBF *10^6	Lambda	Infant Mortality	Corr. Factor	Environment Factor	Net Lambda	Net MTBF	Reliability
Unit	hours	/10^6hours	Parts per million					
Diode Schottkey	250.00	0.00400	10	1.00	0.50	0.00200	500.00	0.99999
2 pin Connector(Power)	142.86	0.00700	0	1.50	0.50	0.00525	190.48	0.99998
2 pin Connector(data)	1000.00	0.00100	0	2.49	0.50	0.00125	801.95	1.00000
UCC3911, series 5 caps, 2res(lp), 30 pin soldering	278.00	0.00360	229	1.00	1.00	0.00360	278.00	0.99996
TPS203x, series 3 caps, 2res(lp), 20 solder joints	2080.00	0.00048	42	1.00	0.50	0.00024	4160.00	0.99997
PTH08080, series 2 tantalum caps, 2 res(lp)	48.00	0.02083	100	1.00	1.00	0.02083	48.00	0.99992
PTR08060, series 2 tantalum caps, 2 res(lp)	13.70	0.07299	100	1.00	1.00	0.07299	13.70	0.99976
Resistor(Low Current)	416.67	0.00240	0	0.14	0.50	0.00016	6127.45	0.99999
Resistor(High Current)	416.67	0.00240	0	0.46	0.50	0.00056	1795.98	0.99999
Tantalum Capacitor	2500.00	0.00040	0	3.30	0.50	0.00066	1515.15	1.00000
Ceramic Capacitor	1000.00	0.00100	0	4.30	0.50	0.00215	465.12	1.00000
PCB with PTH	90.91	0.01100	0	2183.51	0.50	12.00930	0.08	0.99997
Each soldering joint	14285.71	0.00007	100	1.00	0.50	0.00004	28571.43	1.00000
PIC16C77 series 7805, 5 caps, 50pin solder	300.00	0.00333	100	1.00	1.00	0.00333	300.00	0.99996
Sensors	1000.00	0.00100	10	1.00	1.00	0.00100	1000.00	1.00000
UA7805	737	0.00136	10	1.00	1.00	0.00136	737.00	1.00000
Battery	1.54	0.65000		1.00	1.00	0.65000	1.54	0.99806
Solar Panel	0.17	6.00000		1.00	1.00	6.00000	0.17	0.98221

Reliability from Panel + connectors+diode assuming 3of 4 must work	Reliability from Panel + connectors+diode	UCC series battery	UCC series battery one of two must work	pth series diode	pth series diode one of two must work
0.99814	0.98218	0.99798	1.00000	0.99991	1.00000

tps203x series two pin connector	6 tps in series	If redundant tps is used	PCB,uC,sensor in series	Net for circuit
0.99995	0.99970	1.00000	0.99991	0.99771

Conclusion: There is 0.24% probability that the circuit will fail before 4 months

Where the correction factor takes care of following considerations:

Power stress factor for resistors, Series resistance factor for capacitors and complexity factor for Printed circuit boards.

Numbers in red are not justified.

Reliability Analysis in Launch condition

Component	Base Factor	Base MTBF	Environment factor	Other Considerations	Corresponding Factor	Lambda	MTBF	Reliability
Diode Schottkey	0.0040	250.00	33		1.00	0.1320	7.5758	0.999999
2 pin Connector(Power)	0.0070	142.86	36	No. of pins	1.50	0.3780	2.6455	0.999996
2 pin Connector(data)	0.0010	1000.00	36	No. of pins	2.49	0.0898	11.1382	0.999999
UCC3911	0.0036	278.00	50		1.00	0.1799	5.5600	0.999998
TPS203x	0.0005	2080.00	67		1.00	0.0322	31.0448	1.000000
PTH08080	0.0208	48.00	34		1.00	0.7083	1.4118	0.999993
PTR08060	0.0730	13.70	34		1.00	2.4818	0.4029	0.999975
Resistor(Low Current)	0.0024	416.67	87	Power dessipation^0.40, stress factor	0.14	0.0284	35.2152	1.000000
Resistor(High Current, sense)	0.0024	416.67	87	Power dessipation^0.40, stress factor	0.46	0.0969	10.3217	0.999999
Tantalum Capacitor	0.0004	2500.00	50	Series resistance factor, capacitance factor	3.30	0.0660	15.1515	0.999999
Ceramic Capacitor	0.0010	1000.00	50	Series resistance factor, capacitance factor	4.30	0.2150	4.6512	0.999998
PCB with PTH	0.0000	58823.53	27	Complexity, No. of pth to be hand soldered	2183.51	1.0022	0.9978	0.999990
Each soldering joint	0.0001	14285.71	50		1.00	0.0035	285.7143	1.000000
PIC16C77	0.0033	300.00	50		1.00	0.1667	6.0000	0.999998
Sensors	0.0010	1000.00	50		1.00	0.0500	20.0000	1.000000
UA7805	0.0013569	737	50		1.00	0.0678	14.7400	0.999999
Battery	0.6500	1.54	50		1.00	32.5000	0.0308	0.999676
Solar Panel	6.0000	0.17	50		1.00	300.0000	0.0033	0.997014

Reliability from Panel + connectors+diode assuming 3of 4 must work	Rel. Panel + connectors + diode	UCC series battery	UCC series battery one of two must work	pth series diode	pth series diode one of two must work	tps203x series two pin connector	6 tps in series	If redun-dant tps is used
0.99995	0.99701	0.99967	1.00000	0.99999	1.00000	1.00000	0.99998	1.00000

100 soldering Joints	PCB,uC, sensor in series	Net for circuit
1.00000	0.99998	0.99990

Conclusion: There is 0.01% probability that the circuit will fail while in launch

Power Systems Flow-Chart for Engineering Model Code

Main Loop:

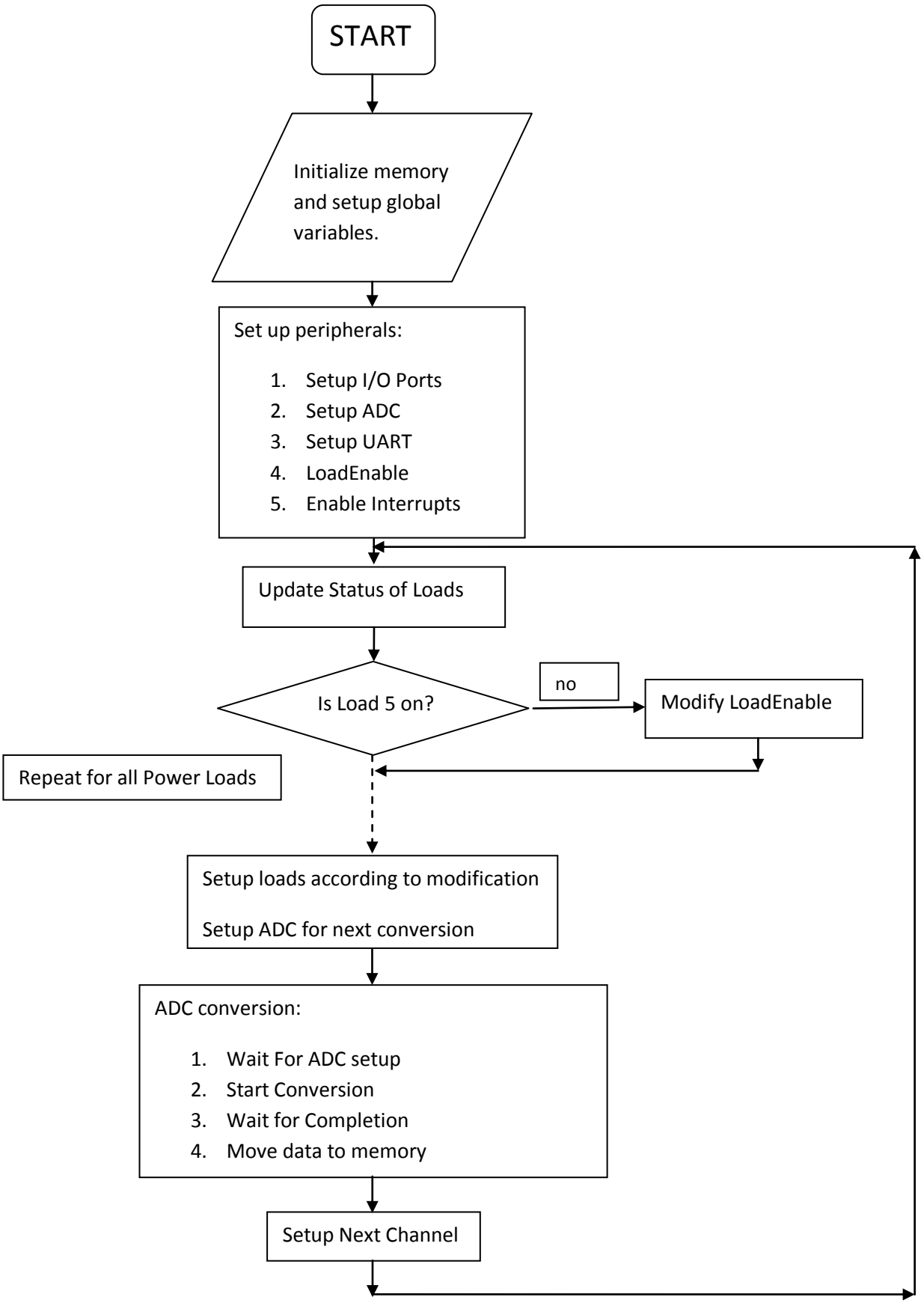

Interrupt Vector: